Polyselenide Chemistry of Indium and Thallium in Dimethylformamide, Acetonitrile, and Water. Syntheses, Structures, and Properties of the New Complexes $[In_2(Se_4)_4(Se_5)]^{4-}$, $[In_2Se_2(Se_4)_2]^{2-}$, $[In_3Se_3(Se_4)_3]^{3-}$, and $[Tl_3Se_3(Se_4)_3]^{3-}$

Sandeep S. Dhingra and Mercouri G. Kanatzidis*

Department of Chemistry and Center for Fundamental Materials Research, Michigan State University, East Lansing, Michigan 48824

Received October 1, 1992

The reaction of $InCl_3$ with Na_2Se_5 in dimethylformamide (DMF) in the presence of Ph_4PCl gave $(Ph_4P)_4[In_2(Se_4)_4(Se_5)]$ (**I**) in 75% yield. Under the same conditions, $InCl_3$ reacted with Na_2Se_5 in the presence of Pr_4NBr or Et_4NBr and afforded $(Pr_4N)_4[In_2(Se_4)_4(Se_5)]$ (**II**) in 65% yield and $(Et_4N)_4[In_2(Se_4)_4(Se_5)]$ (**III**) in 72% yield, respectively. (**I**) crystallizes in the triclinic space group $P\bar{1}$ (No. 2) with unit cell dimensions a = 11.417(4) Å, b = 12.734(9) Å, c = 20.188(9) Å, α = 96.03(5)°, β = 94.69(3)°, γ = 111.68(4)°, V = 2689(2) Å^3, Z = 1, and R/R_w = 0.073/0.085. (**II**) crystallizes in the monoclinic space group $P2/c$ (No. 13) with unit cell dimensions a = 15.997(3) Å, b = 17.376(3) Å, c = 15.168(2) Å, β = 94.56(3)°, V = 4202(1) Å^3, Z = 2, and R/R_w = 0.069/0.080. (**III**) crystallizes in the triclinic space group $P\bar{1}$ (No. 2) with unit cell dimensions a = 12.428(3) Å, b = 15.781(3) Å, c = 17.540(4) Å, α = 89.47(2)°, β = 97.90(2)°, γ = 94.47(2)°, V = 3397(1) Å^3, Z = 2, and R/R_w = 0.075/0.084. Single-crystal X-ray diffraction studies show that (**I**), (**II**), and (**III**) contain the same anion, $[In_2(Se_4)_4(Se_5)]^{4-}$. The anion consists of In^{3+} centers in trigonal bipyramidal coordination; each In atom is chelated by two bidentate Se_4^{2-} ligands forming a $[In(Se_4)_2]^-$ unit. Two of these $[In(Se_4)_2]^-$ units are bridged by an Se_5^{2-} chain forming a dimer. The hydrothermal reaction of $InCl_3$ with Na_2Se_4 in the presence of Pr_4NBr and water at 110 °C for 3 days in an evacuated sealed Pyrex tube afforded deep red crystals of $(Pr_4N)_2[In_2Se_2(Se_4)_2]$ (**IV**), in 80% yield. Under the same conditions the reaction with $[(Ph_3P)_2N]Cl$ yields $[(Ph_3P)_2N]_2[In_2Se_2(Se_4)_2]$ (**V**) in 60% yield. (**IV**) crystallizes in the triclinic space group $P\bar{1}$ (No. 2) with unit cell dimensions a = 8.938(2) Å, b = 11.290(2) Å, c = 11.528(2) Å, α = 79.19(1)°, β = 105.56(1)°, γ = 99.84(1)°, V = 1093(1) Å^3, Z = 1, and R/R_w = 0.045/0.049. (**V**) also crystallizes in the triclinic space group $P\bar{1}$ (No. 2) with unit cell dimensions a = 10.931(5) Å, b = 11.302(7) Å, c = 15.189(8) Å, α = 84.98(5)°, β = 94.15(4)°, γ = 93.86(4)°, V = 1858(1) Å^3, Z = 1, and R/R_w = 0.060/0.081. Single-crystal X-ray diffraction studies show that (**IV**) and (**V**) contain the same binuclear anion $[In_2Se_2(Se_4)_2]^{2-}$. The anion contains In^{3+} with a tetrahedral coordination, bridged by two monoselenides to form a planar $[In_2Se_2]^{2+}$ core with an inversion center at the middle of the In--In vector of 3.336(2) Å. The remaining two coordination sites on each In atom are occupied by the Se_4^{2-} bidentate chelates. The reaction of $InCl_3$ with Na_2Se_5 in 1:2 mole ratio in acetonitrile in the presence of Et_4NBr afforded $(Et_4N)_3[In_3Se_3(Se_4)_3]$ (**VI**). Similar reaction of TlCl with Na_2Se_5 in 1:2 mole ratio in DMF in the presence of Et_4NBr gave $(Et_4N)_3[Tl_3Se_3(Se_4)_3]$ (**VII**). Single-crystal X-ray diffraction studies show that the two compounds (**VI**) and (**VII**) are isostructural and crystallize in the monoclinic space group $P2_1/c$ (No. 14). The unit cell dimensions are a = 16.747(4) Å, b = 13.701(3) Å, c = 22.227(3) Å, β = 94.16(2)°, V = 5086(2) Å^3, Z = 4, and R/R_w = 0.045/0.051 and a = 16.813(3) Å, b = 13.774(3) Å, c = 22.186(4) Å, β = 94.13(1)°; V = 5126(2) Å^3, Z = 4, and R/R_w = 0.072/0.087 for (**VI**) and (**VII**), respectively. The trinuclear anion $[M_3Se_3(Se_4)_3]^{3-}$ (M = In, Tl) in (**VI**) and (**VII**) contains M^{3+} with a tetrahedral coordination. Each M^{3+} center has a chelating Se_4^{2-} ligand and is bridged to the other two M^{3+} centers by monoselenide, Se^{2-}, ligands forming a six-membered $[M_3Se_3]^{3+}$ core. Variable-temperature ^{77}Se NMR spectra of (**I**)–(**VII**) are reported. All indium–polyselenide complexes show the same NMR spectrum at room temperature in DMF suggesting that in solution only one In/Se species exists. UV/vis of (**I**)–(**III**) are similar, with two absorptions at ~450 and ~650 nm, while (**IV**)–(**VII**) have a featureless spectra. The electrochemistry of (**I**) and (**VI**) is reported. The solid-state far-IR spectra of all the compounds show strong absorptions in the 300–100 cm^{-1} region due to the Se–Se and M–Se stretching frequencies; tentative assignments are reported herein. Thermal gravimetric analysis data show that the compounds pyrolyze to give single-phase binary metal chalcogenides (β-In_2Se_3 and TlSe).

Introduction

In recent years the coordination chemistry of soluble metal–polychalcogenides Q_x^{2-} (Q = S, Se, Te) has become an active area of research.[1,2] One reason for this is their remarkable ability to exist in many sizes and participate in various bonding modes, in an extremely large variety of structure types with transition and main group metals. Polychalcogenide complexes now represent one of the most structurally diverse classes in inorganic chemistry. Soluble metal polysulfides have received considerable emphasis due to their importance in fields such as modeling of biological systems,[3] industrial (hydrodesulfurization, HDS) or enzymatic catalysis,[4] lubricants,[5] electrodes in rechargeable batteries,[6] etc.[7] Despite the large number of known polysulfide complexes,[2] the corresponding chemistry of heavier chalcogens

(1) (a) Kanatzidis, M. G. *Comments Inorg. Chem.* **1990**, *10*, 161–195. (b) Ansari, M. A.; Ibers, J. A. *Coord. Chem. Rev.* **1990**, *100*, 223–266. (c) Kolis, J. W. *Coord. Chem. Rev* **1990**, *105*, 195–219.

(2) (a) Draganjac, M.; Rauchfuss, T. B. *Angew. Chem., Int. Ed. Engl.* **1985**, *24*, 742–757. (b) Müller, A. *Polyhedron* **1986**, *5*, 323–340. (c) Müller, A; Diemann, E. *Adv. Inorg. Chem. Radiochem.* **1987**, *31*, 89–122.

(3) Coucouvanis, D. *Acc. Chem. Res.* **1981**, *14*, 201–209.

(4) (a) Chianelli, R. R. *Catal. Rev—Sci. Eng.* **1984**, *26*, 361–393. (b) Holm, R. H.; Simhon, E. D. In *Molybdenum Enzymes*; Spiro, T. G.; Ed.; Wiley-Interscience: New York, 1985; Chapter 1.

(5) Subba Rao, G. V.; Shafer, M. W. In *Intercalated Layered Materials*; Levy, F., Ed. Reidel Publishing Co.: Dordrecht, The Netherlands, p 122.

0020-1669/93/1332-1350$04.00/0

has only recently received attention.[1] Due to the different redox potentials and bond lengths between the various Q–Q bonds the coordination chemistry of the Q_x^{2-} ligands is not entirely analogous in going from S to Se to Te. Even if the structure of a metal polysulfide complex is known, it is not possible to reliably predict the structure of the corresponding polyselenide and polytelluride. The ability to vary x in the Q_x^{2-}, often allows for the synthesis of several different complexes within the same M/Q_x^{2-} system. Some typical polyselenide and polytelluride complexes are: $[Fe_2Se_{12}]^{2-}$,[8] $[W_xSe_y]^{2-}$ ($x = 2$, $y = 9$, 10; $x = 3$, $y = 9$),[9] $[V_2Se_{13}]^{2-}$,[10] $[MQ(Se_4)_2]^{2-}$ (M = Mo, W; Q = O, S, Se),[11] $[M(Se_4)_2]^{2-}$ (M = Mn,[12] Ni,[13,15] Pd,[14] Pt,[14,15] Zn, Cd, Hg,[15,16] Pb[13]), $[Cr_3Q_{24}]^{3-}$ (Q = Se, Te),[17] $[MoSe_9]^{2-}$,[18] $[Hg_2Te_5]^{2-}$,[19] $[Hg_4Te_{12}]^{4-}$,[19] $[NbTe_{10}]^{3-}$,[20] $[Au_2Te_2]^{2-}$,[21] $[Au_2Se_{10}]^{2-}$,[22] $[Au_2Se_5]^{2-}$,[22] $[Au_2Se_6]^{2-}$,[22] $[Hg_7Se_{10}]^{4-}$,[23] $[Hg_7Se_9]_n^{4n-}$,[23] $[Cu_2Se_{14}]^{4-}$,[24] $[M(Se_4)_3]^{2-}$ (M = Pt,[25] Sn[26]), $[AgSe_x]^-$ ($x = 4$, 5),[27] etc.

The scarcity of reports on reactions involving soluble polychalcogenides with main group metals prompted us to undertake a systematic investigation into the synthesis of new polychalcogenide complexes with such elements. Another motivation was our desire to find suitable precursors to semiconducting In_2Se_3, InSe, TlSe and $CuInSe_2$.[28] In this report we present the synthesis and structural and spectroscopic characterization of several new indium and thallium polyselenide complexes: $(Ph_4P)_4[In_2(Se_4)_4(Se_5)]$ (I),[29] $(Pr_4N)_4[In_2(Se_4)_4(Se_5)]$ (II), $(Et_4N)_4[In_2(Se_4)_4(Se_5)]$ (III), $(Pr_4N)_2[In_2Se_2(Se_4)_2]$ (IV), $[(Ph_3P)_2N]_2[In_2Se_2(Se_4)_2]$ (V), $(Et_4N)_3[In_3Se_3(Se_4)_3]$ (VI), and $(Et_4N)_3[Tl_3Se_3(Se_4)_3]$ (VII).

Experimental Section

Reagents. The chemicals in this research were used as obtained commercially: selenium, 99.999% purity, American Smelting and Refining Company, Denver, CO; sodium metal, analytical reagent, Mallinckrodt Inc., Paris, KY; indium(III) chloride, 99.999% purity, Cerac Inc., Milwaukee, WI; thallium(I) chloride, 99% purity, tetraphenylphosphonium chloride (Ph_4PCl), 98% purity, tetrapropylammonium bromide (Pr_4NBr), 97% purity, tetraethylammonium bromide (Et_4NBr), 98% purity, bis(triphenylphosphine) imidium chloride ($[(Ph_3P)_2N]Cl$), 99% purity, Aldrich Chemical Co. Inc., Milwaukee, WI. Dimethylformamide (DMF), analytical reagent, was stored over 4A Linde molecular sieves for over a week and then distilled under reduced pressure at 25–30 °C. The first 50 mL was discarded. Acetonitrile (analytical reagent, Mallinckrodt Inc., Paris, KY) was distilled after refluxing with calcium hydride for 8 h. Diethyl ether (ACS anhydrous, Columbus Chemical Industries Inc., Columbus, WI) was distilled after refluxing with sodium/potassium alloy, with benzophenone and triethylene glycol dimethyl ether for 12 h. Deuterated dimethylformamide-d_7, 99.5 atom % D; acetonitrile-d_3, 99.5 atom % D; and pyridine-d_5, 100 atom % D (Aldrich Chemical Co. Inc., Milwaukee, WI) were used without further purification.

Physicochemical Studies. ^{77}Se ($I = {}^1/_2$, natural abundance 7.58%) NMR spectra were obtained on a Varian VXR-500 (superconducting cryomagnet 11.74 T) pulse spectrometer, equipped with a Sun-3/60 workstation. The spectra were recorded using a broad band 5-mm probe (frequency range 50-202 MHz). The ^{77}Se signal was observed at 95.358 MHz with an acquisition time of 0.322 s. The pulse width in all experiments was 14 μs (i.e. the 90° pulse for this instrument) and no relaxation delay was applied. The number of free induction decays accumulated were ~72 000, and a line broadening of 40 Hz was typically applied. The spectra were referenced to Me_2Se at $\delta = 0$ ppm in DMF and a solution of Ph_2Se_2 ($\delta = 460$ ppm) in DMF was used as an external standard. The convention used for the chemical shifts is that a positive sign signifies a shift to lower field compared to the reference compound. The Varian VXR-500 instrument is equipped with a variable-temperature unit to control the internal temperature of the probe.

Infrared spectra of the complexes were recorded as solids in a CsI matrix on a Nicolet 740 FT-IR spectrometer. Each sample was ground along with CsI to a fine powder and a translucent pellet was made by applying ~15 000 psi pressure to the mixture. The spectra were recorded in the far-IR region (500–100 cm^{-1}). UV/vis spectra of the complexes were measured in solution on a Hitachi U-2000 spectrophotometer.

Thermal gravimetric analyses (TGA) of the compounds were performed on either a Cahn TG system 121 or a Shimadzu TGA-50. The solid samples were heated from room temperature to 800 °C at a rate of 5 °C/min under a steady flow of dry nitrogen.

A three-electrode potentiostat (EG&G Princeton Applied Research Model 273 potentiostat/galvanostat) was used for the cyclic voltammetric experiments. The scans were initiated at the rest potential of each solution under an atmosphere of argon. The working electrode and counter electrode were platinum bead and coil, respectively. The reference electrode was the saturated calomel electrode (SCE). The cyclic voltammetric studies of (I), (II), (VI) and $(Ph_4P)_2Se_5$ are of 2 mmol DMF solutions in 0.1 M n-Bu_4NClO_4.

Quantitative microprobe analysis of the compounds was performed on a scanning electron microscopy (SEM) JEOL JSM-35C equipped with an X-ray microanalysis attachment from Tracor Northern TN 5500, for energy dispersive spectroscopy (EDS). Single crystals of each sample were mounted on an aluminum stub using conductive carbon paint for adhesion to the stub as well as to dissipate charge that is developed on the sample under an electron beam. Energy dispersive spectra were obtained using the following experimental set-up: X-ray detector position: 55 mm; working distance, 39 mm; accelerating voltage, 20 KV, take-off angle, 27 deg; beam current, 200 pA; accumulation time, 60 s; detector window, beryllium. A standardless quantitative (SQ analysis) program was used to analyze the X-ray spectra obtained. The analysis could not be used for atoms below atomic number 11 (sodium) due to the absorption of the low energy X-rays by the Be window of the detector. Since the selenium ratio is always underestimated by this technique, a correction factor (×1.6), which was determined by taking commercial In_2Se_3 as a standard to evaluate the Se ratio. The analysis reported here are an average of three to four individual measurements on several different single crystals of each compound.

Syntheses. All the experiments and syntheses were performed under an atmosphere of dry nitrogen in a Vacuum Atmospheres Dri-Lab glovebox. Elemental analyses on samples (dried under vacuum for 6–8

(6) (a) Rouxel, J.; Brec, R. *Annu. Rev. Mater. Sci.* **1986**, *16*, 137. (b) Whittingham, M.; Tammenmaa, M.; Asplund, M. *Mat. Res. Bull.* **1988**, *23*, 133–142.
(7) (a) Oikkonen, M.; Tammenmaa, M.; Asplund, M. *Mat. Res. Bull.* **1988**, *23*, 133–142. (b) Yamaga, S.; Yoshikawa, A.; Kasai, H. *Jpn. J. Appl. Phys.* **1987**, *26*, 1002. (c) Fonash, S. J. *CRC Crit. Rev. Solid State Mater. Sci.* **1980**, *2*, 107.
(8) Strasdeit, H.; Krebs, B.; Henkel, G. *Inorg. Chim. Acta* **1984**, *89*, L1–L13.
(9) Wardle, R. W. M.; Chau, C.-N.; Ibers, J. A. *J. Am. Chem. Soc.* **1987**, *109*, 1859–1866.
(10) Chau, C.-N.; Wardle, R. W. M.; Ibers, J. A. *Inorg. Chem.* **1987**, *26*, 2740–2741.
(11) Wardle, R. W. M.; Mahler, C. H.; Chau, C.-N.; Ibers, J. A. *Inorg. Chem.* **1988**, *27*, 2790–2795.
(12) (a) O'Neal, S. C.; Pennington, W. T.; Kolis, J. W. *Inorg. Chem.* **1990**, *29*, 3134–3138. (b) Kräuter, G.; Ha-Eierdanz, M.; Müller, U.; Dehnicke, K. *Z. Naturforsch.* **1990**, *45B*, 695–700.
(13) Banda, R. M. H.; Cusick, J.; Scudder, M. L.; Craig, D. C.; Dance, I. G. *Polyhedron* **1989**, *8*, 1995–1998.
(14) Kräuter, G.; Dehnicke, K.; Fenske, D. *Chem.-Ztg.* **1990**, *114*, 7–9.
(15) Ansari, M. A.; Mahler, C. H.; Chorghade, G. S.; Lu, Y.-J.; Ibers, J. A. *Inorg. Chem.* **1990**, *29*, 3832–3839.
(16) (a) Adel, J.; Weller, F.; Dehnicke, K. *Z. Naturforsch.* **1988**, *43B*, 1094–1100. (b) Kanatzidis, M. G. Abstracts of Papers, 196th National Meeting of the American Chemical Society, Los Angeles, CA; American Chemical Society: Washington, DC, 1988, INORG 469. (c) Kräuter, G.; Weller, F.; Dehnicke, K. *Z. Naturforsch.* **1989**, *44B*, 444–454.
(17) Flomer, W. A.; O'Neal, S. C.; Pennington, W. T.; Jeter, D.; Cordes, A. W.; Kolis, J. W. *Angew. Chem., Int. Ed. Engl.* **1988**, *27*, 1702–1703.
(18) O'Neal, S. C.; Kolis, J. W. *J. Am. Chem. Soc.* **1988**, *110*, 1971–1973.
(19) Haushalter, R. C. *Angew. Chem., Int. Ed. Engl.* **1985**, *24*, 433–435.
(20) Flomer, W. A.; Kolis, J. W. *J. Am. Chem. Soc.* **1988**, *110*, 3682–3683.
(21) Haushalter, R. C. *Inorg. Chim. Acta* **1985**, *102*, L37–L38.
(22) (a) Kanatzidis, M. G.; Huang, S.-P. *Inorg. Chem.* **1989**, *28*, 4667–4669. (b) Huang, S.-P.; Kanatzidis, M. G. *Inorg. Chem.* **1991**, *30*, 3572–3575.
(23) Kim, K.-W.; Kanatzidis, M. G. *Inorg. Chem.* **1991**, *30*, 1966–1969.
(24) Müller, U.; Ha-Eierdanz, M.; Kräuter, G.; Dehnicke, K. *Z. Naturforsch.* **1990**, *45B*, 1128–1132.
(25) Ansari, M. A.; Ibers, J. A. *Inorg. Chem.* **1989**, *28*, 4068–4069.
(26) (a) Huang, S.-P.; Dhingra, S.; Kanatzidis, M. G. *Polyhedron* **1990**, *9*, 1389–1395. (b) Banda, R. M. H.; Cusick, J.; Scudder, M. L.; Craig, D. C.; Dance, I. G. *Polyhedron* **1989**, *8*, 1999–2001.
(27) (a) Kanatzidis, M. G.; Huang, S.-P. *J. Am. Chem. Soc.* **1989**, *111*, 760–761. (b) Kanatzidis, M. G.; Huang, S.-P. *Angew. Chem., Int. Ed. Engl.* **1989**, *28*, 1513–1514. (c) Huang, S.-P.; Kanatzidis, M. G. *Inorg. Chem.* **1991**, *30*, 1455–1466.
(28) Dhingra, S.; Kanatzidis M. G. In *Better Ceramics Through Chemistry IV*; *Mat. Res. Soc. Symp. Proc.* **1990**, *180*, 825–830.
(29) Preliminary communication: Kanatzidis, M. G.; Dhingra, S. *Inorg. Chem.* **1989**, *28*, 2024–2026.

h) were performed by Galbraith Analytical Laboratories, Knoxville, TN, and by SEM-EDS studies.

Sodium Pentaselenide, Na_2Se_5. An 18.00-g sample (0.23 mol) of finely powdered elemental selenium was combined with 2.20 g (0.10 mol) of sliced sodium metal in a round bottom flask equipped with a Teflon valve and a stirbar. A 150-mL volume of liquid ammonia was condensed into the flask at −78 °C (dry ice/acetone bath) and the mixture was stirred for a couple of hours until the sodium metal had dissolved completely. When a dark green solution formed, the ammonia was removed by evaporation at room temperature (by allowing the cold bath to warm up slowly) under a steady flow of dry nitrogen. The resulting black solid was dried in vacuum, flame dried and ground to a fine powder in the glovebox. It was used without further characterization. The black powder dissolves in DMF and acetonitrile resulting in deep green solutions but in water, methanol and ethanol gives red solutions.

Preparation of Na_2Se_4 and Na_2Se_6 were accomplished by the same procedure as for Na_2Se_5, by varying the stoichiometric ratios of sodium and selenium accordingly.

Tetrakis(tetraphenylphosphonium) Tetrakis(tetraselenido)(μ_2-pentaselenido)diindate(III), $(Ph_4P)_4[In_2(Se_4)_4(Se_5)]$ (I). To a solution of 0.500 g (1.132 mmol) of Na_2Se_5 and 0.340 g (0.908 mmol) of Ph_4PCl in 60 mL of DMF was added dropwise a 20-mL DMF solution of 0.100 g (0.452 mmol) of $InCl_3$. The mixture was then stirred for ca. 20 min until its color became deep brown-green. Following filtration (to remove NaCl), 100 mL of ether was layered over it to incipient crystallization. Upon standing at room temperature for 2 days, red-brown crystals of $(Ph_4P)_4[In_2(Se_4)_4(Se_5)]$ were formed and isolated by filtration; yield 75%. Anal. Calcd for $C_{96}H_{80}P_4In_2Se_{21}$: C, 34.67; H, 2.41; In, 6.91; Se, 52.27. Found: C, 35.04; H, 2.48; In, 6.86; Se, 50.89.

Tetrakis(tetrapropylammonium) Tetrakis(tetraselenido)(μ_2-pentaselenido)diindate(III), $(Pr_4N)_4[In_2(Se_4)_4(Se_5)]$ (II). To a solution of 0.500 g (1.132 mmol) of Na_2Se_5 and 0.240 g (0.901 mmol) of Pr_4NBr in 60 mL of DMF was added dropwise a 20-mL DMF solution containing 0.100 g (0.452 mmol) of $InCl_3$. There was an immediate reaction resulting in a color change from deep green to brown green. The solution was stirred for ca. 20 min and then filtered to remove NaCl and NaBr. The filtrate was layered with 80 mL of ether to incipient crystallization. Upon standing at room temperature for 2 days brown-red crystals of $(Pr_4N)_4[In_2(Se_4)_4(Se_5)]$ were isolated and washed with ether. Yield: 68%. Anal. Calcd for $C_{48}H_{112}N_4In_2Se_{21}$: C, 21.24; H, 4.13; N, 2.065; In, 8.47. Found: C, 18.98; H, 3.54; N, 1.82; In, 6.78. A quantitative microprobe analysis performed on a number of crystals of (II) with EDS/SEM system gave an average composition of $InSe_{10.1}$.

Tetrakis(tetraethylammonium) Tetrakis(tetraselenido)(μ_2-pentaselenido)diindate(III), $(Et_4N)_4[In_2(Se_4)_4(Se_5)]$ (III). To a solution of 0.500 g (1.132 mmol) of Na_2Se_5 and 0.190 g (0.905 mmol) of Et_4NBr in 60 mL of DMF was added dropwise a 20-mL DMF solution containing 0.100 g (0.452 mmol) of $InCl_3$. There was an immediate reaction resulting in a color change from deep green to brown green. The solution was stirred for ca. 20 min and then filtered to remove NaCl and NaBr. The filtrate was layered with 80 mL of ether to induce crystallization of brown-red crystals of $(Et_4N)_4[In_2(Se_4)_4(Se_5)]$. Yield: 72%. Anal. Calcd for $C_{32}H_{80}N_4In_2Se_{21}$: C, 15.44; H, 3.22; N, 2.25; In, 9.23. Found: C, 16.03; H, 3.13; N, 2.35; In, 8.97.

Bis(tetrapropylammonium) Bis(μ_2-selenido)bis(tetraselenido)diindate(III), $(Pr_4N)_2[In_2Se_2(Se_4)_2]$ (IV). In a Pyrex tube was added 0.050 g (0.226 mmol) of $InCl_3$, 0.164 g (0.453 mmol) of Na_2Se_4 and 0.060 g (0.226 mmol) of Pr_4NBr and 0.5 mL of water. The mixture was frozen in liquid nitrogen and flame sealed under vacuum. The tube was subsequently heated to 110 °C for 3 days. The tube was opened in an inert atmosphere glovebox and the deep red crystals were isolated by filtration, washed with water, ethanol and finally with ether, yield 80%. A quantitative microprobe analysis performed on a number of crystals of (IV) with EDS/SEM system gave an average composition of $InSe_{5.01}$.

Bis(bis(triphenylphosphine) imidium) Bis(μ_2-selenido)bis(tetraselenido)diindate(III), $[(Ph_3P)_2N]_2[In_2Se_2(Se_4)_2]$ (V). In a Pyrex tube was added 0.050 g (0.226 mmol) of $InCl_3$, 0.164 g (0.453 mmol) of Na_2Se_4 and 0.130 g (0.227 mmol) of $[(Ph_3P)_2N]Cl$ and 0.5 mL of water. The procedure was identical to the one for (IV) above. Yield: 60%. A quantitative microprobe analysis performed on a number of crystals of (V) with EDS/SEM system gave an average composition of $InSe_{4.8}$.

Tris(tetraethylammonium) Tris(μ_2-selenido)tris(tetraselenido)triindate(III), $(Et_4N)_3[In_3Se_3(Se_4)_3]$ (VI). Method A. A 20-mL acetonitrile (CH_3CN) solution of 0.100 g (0.452 mmol) of $InCl_3$ was added slowly to a 80-mL CH_3CN solution containing 0.400 g (0.908 mmol) of Na_2Se_5 and 0.100 g (0.476 mmol) of Et_4NBr. The resulting light red-brown solution was filtered to remove NaCl, NaBr and some black green solid. To the filtrate was added 60 mL of ether. Upon standing for 4 days, well-formed deep-red single crystals of $(Et_4N)_3[In_3Se_3(Se_4)_3]$ were formed. They were isolated by filtration and washed with ether; yield 76%. A quantitative microprobe analysis performed on a number of crystals of (VI) with EDS/SEM system gave an average composition of $InSe_{5.13}$.

Method B. In a pyrex tube was added 0.050 g (0.226 mmol) of $InCl_3$, 0.164 g (0.453 mmol) of Na_2Se_4 and 0.049 g (0.233 mmol) of Et_4NBr and 0.5 mL of water. The mixture was frozen in liquid nitrogen and flame sealed under vacuum. The tube was subsequently heated to 110 °C for 3 days. The tube was opened in an inert atmosphere glovebox and big orange crystals were isolated by filtration, washed with water, ethanol and finally with ether, yield 85%. A quantitative microprobe analysis performed on a number of crystals of (VI) with EDS/SEM system gave an average composition of $InSe_{5.2}$.

Tris(tetraethylammonium) Tris(μ_2-selenido)tris(tetraselenido)trithalate(III), $(Et_4N)_3[Tl_3Se_3(Se_4)_3]$ (VII). A 0.200-g amount (0.834 mmol) of TlCl was added to a 80-mL DMF solution containing 0.370 g (0.839 mmol) of Na_2Se_5 and 0.180 g (0.857 mmol) of Et_4NBr. The mixture was stirred for ca. 6 h and the resulting red solution was filtered to remove NaBr and NaCl. To the filtrate was added 60 mL of ether. Upon standing for 6 days deep-red single crystals of $(Et_4N)_3[Tl_3Se_3(Se_4)_3]$ were formed. Yield: 70%. A quantitative microprobe analysis performed on a number of crystals of (VII) with EDS/SEM system gave an average composition of $TlSe_{5.12}$.

X-ray Crystallographic Studies. X-ray powder diffraction patterns were recorded either with a standard Debye–Scherrer powder film camera mounted on a Phillips Norelco XRG-5000 X-ray generator operating at 40 kV/20 mA, or a Phillips XRG-3000 computer-controlled powder diffractometer. Ni-filtered, Cu-radiation was used. *d*-spacings (Å) for all materials were measured on the Phillips XRG-3000. The X-ray powder patterns obtained from the complexes, were in good agreement with those calculated, from the atom coordinates obtained from the X-ray single-crystal diffraction studies, using the program POWD-10.[30] This confirmed the homogeneity and the purity of the complexes, assuming no amorphous phases were present. Calculated and observed *d*-spacings (Å) for all complexes are compiled in the supplementary material. The single crystals of complexes (I), (II), (III), (VI) and (VII) were mounted inside glass capillaries and flame sealed. The crystals of (IV) and (V) were mounted on the tip of a glass fiber with epoxy and covered with Krylon to protect their surface from air. The crystallographic data for (I), (II) and (VI) were collected on Nicolet P3 four-circle automated diffractometer using a θ–2θ step scan mode.[31] The data for (III) and (VII) were collected at Crystallytics Co., Lincoln, NE, by Dr. C. S. Day on a Nicolet diffractometer using an ω–2θ scan mode. The data for (IV) and (V) were collected on Rigaku AFC6S four-circle automated diffractometer with ω–2θ scan technique. Accurate unit cell dimensions were determined from the 2θ, ω, ϕ, χ angles of 15–25 machine-centered reflections. The intensities of three check reflections were monitored every 100–150 reflections and did not show any appreciable loss in their intensities over the data collection period. An empirical absorption correction was applied to all data based on ψ scans for 3–5 ($\chi \sim 90°$) reflections. The structures were solved with direct methods and difference Fourier Synthesis maps and refined with full-matrix least square techniques. An additional absorption correction was applied before anisotropic refinement using DIFABS.[32] The calculations were performed on a VAXstation 2000/3100 computer using the TEXSAN crystallographic software package from Molecular Structure Corp. for (IV) and (V) and the SHELXS-86 and SDP combined package of crystallographic programs[33] for the rest of the complexes. All atoms in the anions were refined anisotropically, while only the nitrogen or phosphorous atoms of the cations were refined anisotropically. The carbon atoms were refined isotropically, while the calculated coordinates of the hydrogen atoms were kept fixed. All the structures consist of discrete, well-separated cations and anions.

(30) Smith, D. K.; Nichols, M. C.; Zolensky, M. E. POWD10: A Fortran IV Program for Calculating X-ray Powder Diffraction Pattern, version 10. Pennsylvania State University, 1983.
(31) Nicolet XRD Corporation: Data Collection Operation Manual, part no. 10062, 1982.
(32) DIFABS: An Empirical Method for Correcting Diffractometer Data for Absorption Correction. Walker, N.; Stuart, D. *Acta Crystallogr.* **1983**, *A39*, 158.
(33) (a) Sheldrick, G. M. In *Crystallographic Computing 3*; Sheldrick, G. M., Kruger, C., Doddard, R., Oxford University Press: Oxford, U.K., 1985, pp 175–189. (b) Frenz, B. A. The Enraf-Nonius CAD4 SDP System. In *Computing in Crystallography*; Delft University Press: Delft, Holland, 1978, pp 64–71.

Table I. Summary of Crystallographic Data for $(Ph_4P)_4[In_2(Se_4)_4(Se_5)]$ (I), $(Pr_4N)_4[In_2(Se_4)_4(Se_5)]$ (II), and $(Et_4N)_4[In_2(Se_4)_4(Se_5)]$ (III)

	I	II	III
formula	$C_{96}H_{80}P_4In_2Se_{21}$	$C_{48}H_{112}N_4In_2Se_{21}$	$C_{32}H_{80}N_4In_2Se_{21}$
fw	3245.22	2633.20	2408.79
cryst color	red-brown	red-brown	red-brown
temp (°C)	23	23	23
a (Å)	11.417(4)	15.997(3)	12.428(3)
b (Å)	12.734(9)	17.376(3)	15.781(3)
c (Å)	20.188(9)	15.168(2)	17.540(4)
α (deg)	96.03(5)	90.00	89.47(2)
β (deg)	94.69(3)	94.56(1)	97.90(2)
γ (deg)	111.68(4)	90.00	94.47(2)
Z, V (Å^3)	1, 2689	2, 4202.9	2, 3397
space group	$P\bar{1}$ (No. 2)	$P2/c$ (No. 13)	$P\bar{1}$ (No. 2)
D_{calc} (g cm^{-3})	2.053	2.081	2.355
μ (cm^{-1}) (Mo Kα)	79.0	95.8	118.4
cryst size (mm)	0.20, 0.42, 0.18	0.40, 0.40, 0.04	0.13, 0.51, 0.60
$2\theta_{max}$ (deg)	44	45	45.8
final R/R_w (%)[a]	7.3/8.5	6.9/8.0	7.5/8.4

[a] $R = \sum||F_o| - |F_c||/\sum|F_o|$. $R_w = \{\sum[w(|F_o| - |F_c|)^2]/\sum[w|F_o|)^2]\}^{1/2}$.

Table II. Summary of Crystallographic Data for $(Pr_4N)_2[In_2Se_2(Se_4)_2]$ (IV) and $[(Ph_3P)_2N]_2[In_2Se_2(Se_4)_2]$ (V)

	IV	V
formula	$C_{24}H_{56}N_2In_2Se_{10}$	$C_{72}H_{60}P_4N_2In_2Se_{10}$
fw	1391.97	2096.42
cryst color	orange-red	red/brown
temp (°C)	23	23
a (Å)	8.938(2)	10.931(5)
b (Å)	11.290(2)	11.302(7)
c (Å)	11.528(2)	15.189(8)
α (deg)	79.19(1)	84.98(5)
β (deg)	105.56(1)	94.15(4)
γ (deg)	99.84(1)	93.86(4)
Z, V (Å^3)	1, 1092.8(3)	1, 1858(1)
space group	$P\bar{1}$ (No. 2)	$P\bar{1}$ (No. 2)
D_{calc} (g cm^{-3})	2.117	1.871
μ (cm^{-1}) (Mo Kα)	93.1	55.8
cryst size (mm)	0.16, 0.12, 0.08	0.24, 0.20, 0.14
$2\theta_{max}$ (deg)	45	40
final R/R_w (%)[a]	4.5/4.9	6.0/8.1

[a] $R = \sum||F_o| - |F_c||/\sum|F_o|$. $R_w = \{\sum[w(|F_o| - |F_c|)^2]/\sum[w|F_o|)^2]\}^{1/2}$.

Table III. Summary of Crystallographic Data for $(Et_4N)_3[In_3Se_3(Se_4)_3]$ (VI) and $(Et_4N)_3[Tl_3Se_3(Se_4)_3]$ (VII)

	VI	VII
formula	$C_{24}H_{60}N_3In_3Se_{15}$	$C_{24}H_{60}N_3Tl_3Se_{15}$
fw	1919.63	2188.28
cryst color	deep red	deep red
temp (°C)	23	21
a (Å)	16.747(4)	16.813(3)
b (Å)	13.701(3)	13.774(3)
c (Å)	22.227(3)	22.186(4)
α (deg)	90.00	90.00
β (deg)	94.16(2)	94.13(1)
γ (deg)	90.00	90.00
Z, V (Å^3)	4, 5086.4	4, 5126
space group	$P2_1/c$ (No. 14)	$P2_1/c$ (No. 14)
D_{calc} (g cm^{-3})	2.507	2.835
μ (cm^{-1}) (Mo Kα)	119.8	200.8
cryst size (mm)	0.76, 0.23, 0.40	0.08, 0.36, 0.70
$2\theta_{max}$ (deg)	40	45.8
final R/R_w (%)[a]	4.5/5.1	7.2/8.7

[a] $R = \sum||F_o| - |F_c||/\sum|F_o|$. $R_w = \{\sum[w(|F_o| - |F_c|)^2]/\sum[w|F_o|)^2]\}^{1/2}$.

In $(Pr_4N)_4[In_2(Se_4)_4(Se_5)]$ (II), all cations are situated on special positions. The nitrogen atoms are situated on a 2-fold rotational axes, giving four half-cations in the asymmetric unit. There is disorder in one of the Pr_4N^+ cations, where the middle carbon atoms of the propyl chains are in two different sites of half-occupancy. In this structure there is also disorder in the Se_5^{2-} chain bridging the In atoms. The second selenium atom in the chain Se(10) is positionally disordered over two sites with equal occupancy. The Se(11) atom is disordered over two positions each with half occupancy. This leads to two different conformations of the Se_5^{2-} in the solid state. The Se_5^{2-} chains consist either of the Se(9)Se(10)–Se(11)Se(10)′Se(9) or Se(9)Se(10)′Se(11)′Se(10)Se(9) sequence of atoms.

In $(Pr_4N)_2[In_2Se_2(Se_4)_2]$ (IV) the Pr_4N^+ cation is disordered. The propyl chains have two conformations, the inner two carbon atoms on each of the four chains are positionally disordered over two sites with 0.6 and 0.4 occupancy but the terminal carbon has full occupancy.

In $(Et_4N)_3[In_3Se_3(Se_4)_3]$ (VI) there is disorder in one of the Se_4^{2-} ligands chelating to In(2) atom, thus leading to two different conformations of the $[InSe_4]^+$ five-membered ring. This disorder involves three of the four Se atoms giving two separate Se_4^{2-} ligands: Se(6)Se(7)Se(8)Se(9) and Se(6)Se(7′)Se(8′)Se(9′); see appropriate figure below. The former conformation is the more predominant with 0.7 occupancy. In this structure all the Et_4N^+ cations are disordered with the inner carbon atoms of all the ethyl groups distributed over two different sites of half-occupancy. There is no disorder in the terminal carbons or the nitrogen atoms of the cations.

The complete data collection parameters and details of the structure solution and refinement for all the compounds are summarized in Tables I–III. The final coordinates, temperature factors and their estimated standard deviations (esd's) of all atoms in the anions for all compounds are shown in Tables IV–X.

Results and Discussion

Syntheses. The syntheses of (I)–(III) were accomplished by the reaction between $InCl_3$ and Na_2Se_5, in 2:5 molar ratio, in the presence of various quaternary ammonium or phosphonium cations in DMF, as represented in eq 1.

$$2InCl_3 + 5Na_2Se_5 + 4R_4EX \xrightarrow{DMF} (R_4E)_4[In_2(Se_4)_4(Se_5)] + 4NaX + 6NaCl \quad (1)$$

R = Et, Pr, E = N; R = phenyl, E = P; X = Cl, Br

Initially, the reactions between $InCl_3$ and Na_2Se_5 were run in the 1:2 ratio hoping to obtain $[In(Se_4)_2]^-$, the isostructural complex to $[M(Se_4)_2]^{2-}$ (M = Zn, Cd, Hg).[15,16] Though this complex has not been isolated yet, we found that it is the $[In_2(Se_4)_4(Se_5)]^{4-}$ anion which displays considerable ability to crystallize out in good yield. In addition, a slight variation of the composition of Na_2Se_x (x = 4–6) used or in the $InCl_3$:Na_2Se_5 ratio did not affect the course of the reaction, producing the same $[In_2(Se_4)_4(Se_5)]^{4-}$ in lower yield. The highest yields were obtained by $InCl_3$ to Na_2Se_5 molar ratio of 2:5.

Often the structure of metal polychalcogenide complexes is highly influenced by the nature of the counterions. This has been seen in the Ag/Se_x^{2-},[27] Cu/S_x^{2-},[34] and Mo/S_x^{2-} [35] systems

(34) Müller, A.; Schimanski, U. *Inorg. Chim. Acta* **1983**, *77*, L187.
(35) Hadjikyriacou, A. I.; Coucouvanis, D. *Inorg. Chem.* **1987**, *26*, 2400–2408.

Table IV. Fractional Atomic Coordinates and B_{eq} Values for the Anion in $(Ph_4P)_4[In_2(Se_4)_4(Se_5)]$ (I) with Their Estimated Standard Deviations in Parentheses

atom	x	y	z	B_{eq},[a] Å^2
In	0.3120(2)	0.5934(2)	0.7867(1)	5.07(7)
Se(1)	0.4910(4)	0.7685(3)	0.7465(2)	5.1(1)
Se(2)	0.6609(4)	0.7097(4)	0.7404(2)	7.3(1)
Se(3)	0.5540(4)	0.5169(3)	0.6968(2)	7.5(1)
Se(4)	0.4451(4)	0.4541(3)	0.7879(2)	7.5(1)
Se(5)	0.1491(4)	0.4320(3)	0.6958(2)	6.6(1)
Se(6)	0.0155(5)	0.5151(4)	0.6535(2)	8.7(2)
Se(7)	−0.0110(4)	0.6156(4)	0.7481(3)	8.1(1)
Se(8)	0.1956(4)	0.7463(4)	0.7863(4)	11.5(2)
Se(9)	0.2727(4)	0.5826(5)	0.9121(2)	9.11(2)
Se(10)	0.3435(6)	0.4372(4)	0.9410(2)	10.5(2)
Se(11)	0.4517(8)	0.4768(7)	0.0489(4)	6.5(2)

[a] Anisotropically refined atoms are given in the form of the isotropic equivalent displacement parameter defined as $B_{eq} = (4/3)[a^2B_{11} + b^2B_{22} + c^2B_{33} + ab(\cos\gamma)B_{12} + ac(\cos\beta)B_{13} + bc(\cos\alpha)B_{23}]$.

Table V. Fractional Atomic Coordinates and B_{eq} Values for the Anion in $(Pr_4N)_4[In_2(Se_4)_4(Se_5)]$ (II) with Their Estimated Standard Deviations in Parentheses

atom	x	y	z	B_{eq},[a] Å^2
In	0.7480(2)	0.7567(1)	0.0359(2)	4.22(6)
Se(1)	0.8083(3)	0.7559(2)	−0.1309(2)	5.1(1)
Se(2)	0.7065(3)	0.6848(2)	−0.2013(2)	5.9(1)
Se(3)	0.6452(3)	0.6149(2)	−0.0822(3)	5.9(1)
Se(4)	0.5901(3)	0.7122(2)	0.0107(2)	4.68(9)
Se(5)	0.7981(3)	0.6297(2)	0.1062(3)	6.1(1)
Se(6)	0.8854(3)	0.6859(3)	0.2030(3)	6.6(1)
Se(7)	0.9830(3)	0.7408(3)	0.1048(3)	7.2(1)
Se(8)	0.9048(3)	0.8351(3)	0.0383(3)	6.5(1)
Se(9)	0.7037(3)	0.8764(3)	0.1348(3)	6.8(1)
Se(10)	0.5519(7)	0.8648(6)	0.1473(6)	10.1(3)
Se(10′)	0.4324(6)	0.8987(5)	0.3871(5)	7.4(2)
Se(11)	0.5116(7)	0.8131(5)	0.2962(7)	8.5(3)

[a] Anisotropically refined atoms are given in the form of the isotropic equivalent displacement parameter defined as $B_{eq} = (4/3)[a^2B_{11} + b^2B_{22} + c^2B_{33} + ab(\cos\gamma)B_{12} + ac(\cos\beta)B_{13} + bc(\cos\alpha)B_{23}]$.

to name but a few. This dependence on counterion was probed but was not observed in this study, as the same $[In_2(Se_4)_4(Se_5)]^{4-}$ complex was isolated with three different cations (Ph_4P^+, Pr_4N^+, and Et_4N^+) in DMF.

Surprisingly, when we used CH_3CN as solvent, in the presence of Et_4NBr we isolated a different compound, (**VI**), according to eq 2.

$$InCl_3 + 2Na_2Se_5 + Et_4NBr \xrightarrow{CH_3CN} {}^1/_3(Et_4N)_3[In_3Se_3(Se_4)_3] + 3NaCl + NaBr + 5Se \quad (2)$$

(**VI**) can be dissolved in DMF to give an orange-red solution and can be easily recrystallized unchanged by addition of anhydrous ether.

Since by merely changing the solvent from DMF to CH_3CN we were able to isolate a structurally different anion $[In_3Se_3(Se_4)_3]^{3-}$, we concluded that the final products were strongly influenced by their crystallization properties. This means that isolated products are the least soluble compounds in the given solvent. We thus changed the solvent further and used water. Due to the insufficient solubility of organic salts in water we used the hydrothermal technique. Recently, it has been shown by our group that hydrothermal synthesis can be applied to the preparation of some novel transition and main group metal polychalcogenides.[36-38] In extending this new approach we explored hydrothermal reactions between $InCl_3$ and Na_2Se_5 in various ratios in the presence of different organic counterions in evacuated sealed Pyrex tubes at 110 °C. The synthesis of (**IV**) and (**V**) was accomplished via such hydrothermal reactions of $InCl_3$ and Na_2Se_4 in the presence of Pr_4NBr (eq 3a) or $[(Ph_3P)_2N]Cl$ (eq 3b). Interestingly, Et_4NCl crystallizes the $[In_3Se_3(Se_4)_3]^{3-}$ anion.

Table VI. Fractional Atomic Coordinates and B_{eq} Values for the Anion in $(Et_4N)_4[In_2(Se_4)_4(Se_5)]$ (III) with Their Estimated Standard Deviations in Parentheses

atom	x	y	z	B_{eq},[a] Å^2
In(1)	0.7601(2)	0.7571(1)	0.1065(1)	3.80(4)
In(2)	0.7486(2)	0.2590(1)	0.3931(1)	4.96(5)
Se(1)	0.6834(3)	0.8279(2)	−0.0224(2)	5.40(8)
Se(2)	0.8434(3)	0.8791(3)	−0.0702(2)	6.9(1)
Se(3)	0.9616(3)	0.9106(2)	0.0424(2)	5.87(9)
Se(4)	0.9741(3)	0.7773(2)	0.0986(2)	5.68(8)
Se(5)	0.7671(3)	0.8654(2)	0.2189(2)	6.11(9)
Se(6)	0.5872(3)	0.8993(2)	0.2013(3)	7.5(1)
Se(7)	0.4927(3)	0.7670(3)	0.2031(2)	7.1(1)
Se(8)	0.5309(3)	0.7021(2)	0.0923(2)	5.68(9)
Se(9)	0.7538(3)	0.5932(2)	0.1279(2)	5.47(8)
Se(10)	0.9383(3)	0.5652(3)	0.1390(3)	9.5(1)
Se(11)	0.9844(3)	0.5190(3)	0.2651(3)	7.7(1)
Se(12)	0.9319(3)	0.3755(2)	0.2615(2)	6.82(9)
Se(13)	0.7467(3)	0.3654(2)	0.2782(2)	5.82(8)
Se(14)	0.9541(3)	0.2171(2)	0.3859(2)	5.53(8)
Se(15)	0.9393(4)	0.0901(2)	0.4539(2)	8.0(1)
Se(16)	0.7921(5)	0.0180(3)	0.3779(3)	11.5(2)
Se(17)	0.6514(4)	0.1059(3)	0.3904(2)	8.6(1)
Se(18)	0.8019(3)	0.3320(3)	0.5282(2)	6.9(1)
Se(19)	0.6361(4)	0.3567(4)	0.5654(3)	10.7(1)
Se(20)	0.5403(4)	0.4078(3)	0.4543(3)	11.3(1)
Se(21)	0.5274(3)	0.2922(4)	0.3716(3)	11.0(2)

[a] Anisotropically refined atoms are given in the form of the isotropic equivalent displacement parameter defined as $B_{eq} = (4/3)[a^2B_{11} + b^2B_{22} + c^2B_{33} + ab(\cos\gamma)B_{12} + ac(\cos\beta)B_{13} + bc(\cos\alpha)B_{23}]$.

Table VII. Fractional Atomic Coordinates and B_{eq} Values for the Anion in $(Pr_4N)_2[In_2Se_2(Se_4)_2]$ (IV) with Their Estimated Standard Deviations in Parentheses

atom	x	y	z	B_{eq},[a] Å^2
In(1)	0.5027(1)	0.1313(1)	0.9054(1)	4.11(6)
Se(1)	0.7261(2)	0.0091(2)	1.0281(2)	4.74(9)
Se(2)	0.5676(3)	0.3539(2)	0.9515(2)	6.6(1)
Se(3)	0.4234(3)	0.4405(2)	0.7648(3)	9.2(1)
Se(4)	0.5230(3)	0.3618(2)	0.6311(2)	8.7(1)
Se(5)	0.4279(3)	0.1575(2)	0.6680(2)	6.7(1)

[a] Anisotropically refined atoms are given in the form of the isotropic equivalent displacement parameter defined as $B_{eq} = (4/3)[a^2B_{11} + b^2B_{22} + c^2B_{33} + ab(\cos\gamma)B_{12} + ac(\cos\beta)B_{13} + bc(\cos\alpha)B_{23}]$.

$$InCl_3 + 3Na_2Se_4 + Pr_4NBr \xrightarrow{water} {}^1/_2(Pr_4N)_2[In_2Se_2(Se_4)_2] + NaBr + 3NaCl + Na_2Se_2 \quad (3a)$$

$$[(Ph_3P)_2N]Cl \rightarrow [(Ph_3P)_2N]_2[In_2Se_2(Se_4)_2] \quad (3b)$$

The synthesis of $[Tl_3Se_3(Se_4)_3]^{3-}$ (**VII**) was readily accomplished by stirring a reaction mixture of TlCl and Na_2Se_5 in the presence of Et_4NBr in DMF for several hours as shown in eq 4.

$$TlCl + Na_2Se_5 + Et_4NBr \xrightarrow{DMF} {}^1/_3(Et_4N)_3[Tl_3Se_3(Se_4)_3] + NaCl + NaBr \quad (4)$$

(36) (a) Liao, J.-H.; Kanatzidis, M. G. *J. Am. Chem. Soc.* **1990**, *112*, 7400–7402. (b) Liao, J.-H.; Kanatzidis, M. G. *Inorg. Chem.* **1992**, *31*, 431–439. (c) Kim, K.-W.; Kanatzidis, M. G. *J. Am. Chem. Soc.* **1992**, *114*, 4878–4882

(37) (a) Sheldrick, W. S. *Z. Anorg. Allg. Chem.* **1988**, *562*, 23–30. (b) Sheldrick W. S.; Hauser, H.-J. *Z. Anorg. Allg. Chem.* **1988**, *557*, 98–104. (c) Sheldrick W. S.; Hauser, H.-J. *Z. Anorg. Allg. Chem.* **1988**, *557*, 105–111. (d) Sheldrick, W. S.; Kaub J. *Z. Anorg. Allg. Chem.* **1986**, *535*, 179–185. (e) Sheldrick, W. S.; Braunbeck, H. G. *Z. Naturforsch* **1989**, *44b*, 851–852. (f) Sheldrick, W. S. *Z. Naturforsch* **1988**, *43b*, 249–252.

(38) Parise, J. B. *Science* **1991**, *251*, 293–294. (b) Parise, J. B. *J. Chem. Soc., Chem. Commun.* **1990**, 1553–1554.

Table VIII. Fractional Atomic Coordinates and B_{eq} Values for the Anion in $[(Ph_3P)_2N]_2[In_2Se_2(Se_4)_2]$ (V) with Their Estimated Standard Deviations in Parentheses

atom	x	y	z	B_{eq},[a] Å^2
In(1)	0.5015(2)	0.4155(2)	0.9150(1)	3.5(1)
Se(1)	0.6656(2)	0.4571(3)	1.0390(2)	4.3(2)
Se(2)	0.5398(3)	0.4930(3)	0.7513(2)	6.1(2)
Se(3)	0.5396(3)	0.3124(4)	0.6888(2)	6.8(2)
Se(4)	0.3880(3)	0.1961(3)	0.7590(2)	6.1(2)
Se(5)	0.4624(3)	0.1867(3)	0.9063(2)	5.6(2)

[a] Anisotropically refined atoms are given in the form of the isotropic equivalent displacement parameter defined as $B_{eq} = (4/3)[a^2B_{11} + b^2B_{22} + c^2B_{33} + ab(\cos\gamma)B_{12} + ac(\cos\beta)B_{13} + bc(\cos\alpha)B_{23}]$.

Table IX. Fractional Atomic Coordinates and B_{eq} Values for the Anion in $(Et_4N)_3[In_3Se_3(Se_4)_3]$ (VI) with Their Estimated Standard Deviations in Parentheses

atom	x	y	z	B_{eq},[a] Å^2
In(1)	0.3662(1)	0.2408(1)	0.33395(7)	3.20(4)
In(2)	0.8251(1)	0.6534(1)	0.11634(9)	4.96(5)
In(3)	0.3050(1)	-0.0000(1)	0.28633(7)	3.29(4)
Se(1)	0.2492(2)	0.3436(2)	0.2811(1)	4.27(6)
Se(2)	0.2861(2)	0.4943(2)	0.3248(1)	5.43(7)
Se(3)	0.4227(2)	0.4996(2)	0.3112(1)	5.47(7)
Se(4)	0.4697(2)	0.3715(2)	0.3735(1)	4.70(6)
Se(5)	0.6806(2)	0.6525(2)	0.0725(1)	4.12(6)
Se(6)	0.1090(2)	0.3278(2)	0.3799(1)	5.43(7)
Se(7′)	-0.0005(8)	0.304(1)	0.4324(6)	9.6(4)
Se(7)	0.0247(3)	0.3119(4)	0.4632(2)	6.8(1)
Se(8)	0.0172(3)	0.6510(4)	0.0468(3)	7.9(1)
Se(8′)	0.9551(9)	0.684(1)	0.0012(6)	11.8(4)
Se(9)	0.8953(3)	0.5688(4)	0.0281(2)	8.8(1)
Se(9′)	0.9312(6)	0.5527(8)	0.0589(5)	7.0(3)
Se(10)	0.8356(2)	0.5773(2)	0.2221(1)	5.37(7)
Se(11)	0.6532(2)	0.4127(2)	0.1126(1)	4.85(7)
Se(12)	0.3646(2)	0.7513(2)	0.3526(1)	5.39(7)
Se(13)	0.5871(2)	0.2784(2)	0.2412(1)	5.07(7)
Se(14)	0.6983(2)	0.3545(2)	0.2896(1)	5.09(7)
Se(15)	0.5849(2)	0.6187(2)	0.2409(1)	3.90(6)

[a] Anisotropically refined atoms are given in the form of the isotropic equivalent displacement parameter defined as $B_{eq} = (4/3)[a^2B_{11} + b^2B_{22} + c^2B_{33} + ab(\cos\gamma)B_{12} + ac(\cos\beta)B_{13} + bc(\cos\alpha)B_{23}]$.

To the best our knowledge, $[Tl_3Se_3(Se_4)_3]^{3-}$ is the first thallium polyselenide complex isolated to date. This is a Tl^{3+} complex formed by redox chemistry. The formation of Tl^{3+} by internal electron transfer is unexpected but it is similar to that found in the Au/Se_x^{2-} system.[22] Interestingly, the oxidation potential Au^+ and Tl^+ are very similar (-1.29 and -1.247 V, respectively).[39] The high negative value of the redox potential of Tl^+ is consistent with reductive cleavage of the Se--Se bond in Se_5^{2-}. The formation of (VII) can be rationalized by assuming that the initial step in the reaction is a simple coordination of the Se_5^{2-} ligand to the Tl^+ center, followed by cyclization to give an intermediate trimeric complex, as shown in Figure 1. The cyclic $[Tl_3(Se_5)_3]^{3-}$ structure of the Tl^+ intermediate is homologous to the dimeric anion $[Tl_2(S_4)_2]^{2-}$ [40] and similar to the trimeric Cu^+ polysulfide complex $[Cu_3(S_6)_3]^{3-}$.[34] The formation of Tl^{3+} can be envisioned via internal two electron transfer from the thallium atom to the nearest Se--Se bond of a Se_5^{2-} ligand, thereby generating a Se^{2-} ligand. A subsequent slight rearrangement of the structure results in (VII). This is schematically represented in Figure 1.

Solution Properties. UV/Vis Spectroscopy. The UV/vis spectrum of (I) in DMF is shown in Figure 2A, and features two absorptions at 450 (sh) nm (ϵ = 12 855 cm^{-1} M^{-1}) and 649 nm (ϵ = 2789 cm^{-1} M^{-1}), respectively, while solid-state samples (KBr pellet) show only a featureless rising absorbance. In DMF (I)–(III) containing the $[In_2(Se_4)_4(Se_5)]^{4-}$ anion have similar UV/vis spectra and also resemble those of Na_2Se_5 and $(Ph_4P)_2Se_5$ in the same solvent. The UV/vis spectrum of the Se_5^{2-} in DMF is shown in Figure 2B and is similar to those of (I)–(III) indicating that these anions dissociate in DMF giving rise to Se_x^{2-} species. The two absorption bands can be attributed to the presence of possible selenium radical anion species[1a] such as $Se_3^{\bullet-}$ in equilibrium with Se_x^{2-} anions by analogy to the polysulfides.[41]

The UV/vis spectra of $[In_2Se_2(Se_4)_2]^{2-}$ in (IV) and (V) as well as the $[M_3Se_3(Se_4)_3]^{3-}$ (M = In, Tl) in (VI) and (VII) in DMF are featureless indicating that these compounds do not yield Se_x^{2-} species, Figure 2C.

Cyclic Voltammetric Studies. The presence of Se_x^{2-} species in the DMF solutions of (I)–(III) are further supported by cyclic voltammetric studies. The cyclic voltammogram of (I) shows an irreversible oxidation wave at -0.35 V which is followed by two reduction waves at -0.82 and -1.25 V vs saturated calomel electrode (SCE). The latter two reduction waves are seen only after the former oxidation wave has ensued and hence are not due to species originally present in the solution, Figure 3. In comparison, $(Ph_4P)_2Se_5$ gives qualitatively similar cyclic voltammograms in DMF, an irreversible oxidation wave at -0.42 V followed by two reduction waves at -0.71 and -1.14 V, respectively. This Se_5^{2-} solution shows similar behavior, the reduction waves are seen only after the oxidation wave as in (I) and (II), thus indicating that the redox-active species in the DMF solutions are similar.

Table X. Fractional Atomic Coordinates and B_{eq} Values for the Anion in $(Et_4N)_3[Tl_3Se_3(Se_4)_3]$ (VII) with Their Estimated Standard Deviations in Parentheses

atom	x	y	z	B_{eq},[a] Å^2
Tl(1)	0.6317	0.2576	0.16664	2.98
Tl(2)	0.6959	0.4995	0.21703	3.01
Tl(3)	0.8244	0.3473	0.11320	4.74
Se(1)	0.7521	0.1526	0.2181	4.0
Se(2)	0.7141	0.0027	0.1742	5.2
Se(3)	0.5782	-0.0041	0.1888	5.0
Se(4)	0.5298	0.1207	0.1260	4.4
Se(5)	0.5820	0.3796	0.2435	3.7
Se(6)	0.6947	0.6515	0.2915	4.6
Se(7)	0.5841	0.7224	0.2403	4.9
Se(8)	0.6329	0.7460	0.1468	5.5
Se(9)	0.6486	0.5849	0.1127	4.6
Se(10)	0.8379	0.4189	0.2232	5.4
Se(11)	0.9068	0.4339	0.0298	11.6
Se(12)	1.0187	0.3425	0.0423	11.0
Se(13)	0.9769	0.1857	0.0380	8.8
Se(14)	0.8903	0.1695	0.1171	5.0
Se(15)	0.6773	0.3490	0.0699	4.0

[a] Anisotropically refined atoms are given in the form of the isotropic equivalent displacement parameter defined as $B_{eq} = (4/3)[a^2B_{11} + b^2B_{22} + c^2B_{33} + ab(\cos\gamma)B_{12} + ac(\cos\beta)B_{13} + bc(\cos\alpha)B_{23}]$.

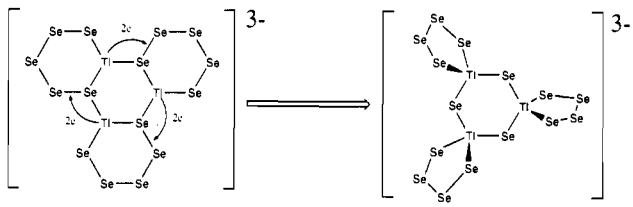

Figure 1. Schematic showing possible species involved the redox chemistry between Tl^+ and Se_5^{2-} and formation of $[Tl_3Se_3(Se_4)_3]^{3-}$.

(39) *Electrochemical Methods, Fundamentals and Applications*; Bard, A. J., Faulkner, L. R., Eds.; John Wiley & Sons: New York, 1980, pp 700–701.

(40) Dhingra, S.; Kanatzidis, M. G. *Inorg. Chem.*, in press.

(41) The UV/vis, Raman and resonance Raman spectroscopic studies on polysulfides in liquid ammonia or polar solvents such as DMF suggest that different S_x^{2-} ligands are in equilibrium with the radical anion $S_3^{\bullet-}$ and other species such as $S_2^{\bullet-}$. However, the existence of $Se^{\bullet-}$ radicals has not yet been unequivocally established. (a) Dubois, P.; Lelieur, J. P.; Lepourte, G. *Inorg. Chem.* **1988**, *27*, 73–80. (b) Clark, R. J. H.; Walton, J. R. *J. Chem. Soc., Dalton Trans.* **1987**, 1535–1544. (b) Clark, R. J. H.; Dines, T. J.; Proud, G. P. *J. Chem. Soc., Dalton Trans.* **1983**, 2299–2302.

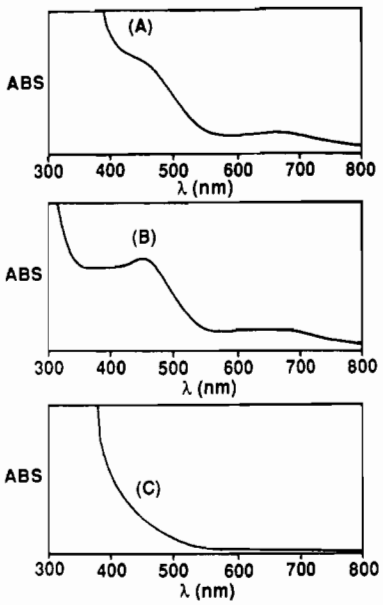

Figure 2. Typical UV/vis spectra of (A) $(Ph_4P)_4[In_2(Se_4)_4(Se_5)]$ (I), (B) $(Ph_4P)_2Se_5$, and (C) $(Et_4N)_3[In_3Se_3(Se_4)_3]$ (VI) in DMF.

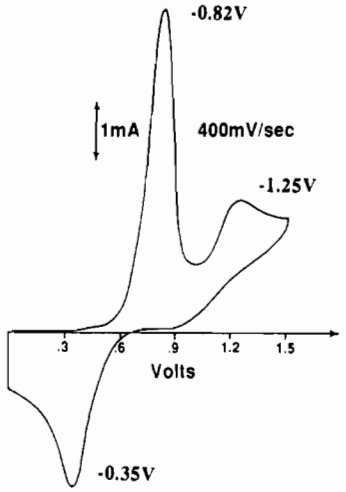

Figure 3. Cyclic voltammogram of $(Ph_4P)_4[In_2(Se_4)_4(Se_5)]$(I) in DMF. (II) and (III) as well as $(Ph_4P)_2Se_5$ have similar voltammograms.

The cyclic voltammogram of $(Et_4N)_3[In_3Se_3(Se_4)_3]$ in CH_3CN shows an irreversible reduction wave at –1.31 V in the first cycle and an irreversible oxidation wave at –0.57 V (at 200 mV/s). Further cycles show a new reduction wave at –1.03 V while the reduction wave at –1.31 V disappears. The oxidation wave at –0.57 V remains unchanged. These redox waves are associated with reductive cleavage (–1.31 V) and oxidative formation (–0.57 V) of Se–Se bonds.

^{77}Se NMR Studies. The ^{77}Se NMR spectra of (I)–(III) in DMF solutions at room temperature and at –55 °C are identical and show three peaks in 2:2:1 ratio at 643 ppm, 197 ppm and –244 ppm, respectively; see Figure 4. Interestingly, the ^{77}Se NMR spectra of $[In_3Se_3(Se_4)_3]^{3-}$ in DMF or CH_3CN solutions are also identical to those of $[In_2(Se_4)_4(Se_5)]^{4-}$. Based on the structure of $[In_3Se_3(Se_4)_3]^{3-}$ and on the assumption that there is a conformational lability in solution (giving rise to a 3-fold axis in the molecule), three distinct peaks are expected in its ^{77}Se NMR spectrum. Surprisingly, the ^{77}Se NMR spectra of $[In_2Se_2(Se_4)_2]^{2-}$ in DMF solutions are identical to those of $[In_2(Se_4)_4(Se_5)]^{4-}$ and $[In_3Se_3(Se_4)_3]^{3-}$ as well. The peak at 643 ppm can be tentatively assigned to resonance from the terminal Se atoms of the chelating Se_4^{2-} ligands and 197 ppm from the inner atoms of the Se_4^{2-} ligands while the –244 ppm is more reasonably assigned to the bridging Se^{2-} ligand. This assignment is consistent with the ^{77}Se

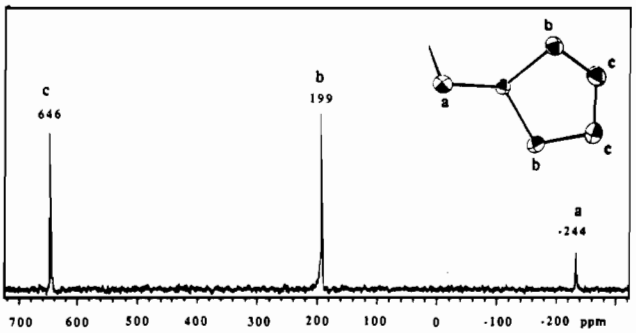

Figure 4. The common ^{77}Se NMR spectrum of $(Ph_4P)_4[In_2(Se_4)_4(Se_5)]$ (I), $(Pr_4N)_2[In_2Se_2(Se_4)_2]$ (IV), and $(Et_4N)_3[In_3Se_3(Se_4)_3]$ (VI) in DMF. Inset: Schematic assignment of the peaks.

NMR results from similar metal polyselenide complexes reported recently.[15] Under our experimental conditions we found no evidence of any satellite peaks arising from In--Se coupling (^{115}In has $I = {}^9/_2$, natural abundance 95.8%). The fact that the ^{77}Se NMR spectra of all the In/Se_x complexes are identical in DMF, coupled with the lability of $[In_2(Se_4)_4(Se_5)]^{4-}$ suggest a possible equilibrium between this complex and $[In_nSe_n(Se_4)_n]^{n-}$, (n = 2, 3) as shown in eqs 5–7.

$$3[In_2(Se_4)_4(Se_5)]^{4-} \leftrightarrow 2[In_3Se_3(Se_4)_3]^{3-} + 3Se_{11}^{2-} \quad (5)$$

$$[In_2(Se_4)_4(Se_5)]^{4-} \leftrightarrow [In_2Se_2(Se_4)_2]^{2-} + Se_{11}^{2-} \quad (6)$$

$$2Se_{11}^{2-} \leftrightarrow Se_x^{2-} + Se_y^{2-} \qquad x + y = 22 \quad (7)$$

The identical ^{77}Se NMR spectra of $[In_2Se_2(Se_4)_2]^{2-}$ and $[In_3Se_3(Se_4)_3]^{3-}$ in DMF suggest that only one indium–polyselenide complex exists in solution. The question is which? Intuitively, one would expect the dimeric $[In_2Se_2(Se_4)_2]^{2-}$ to possess higher energy ring-strain compared to the trimeric homologue, and therefore anticipate the latter to be the final solution product. Another destabilizing factor for the $[In_2Se_2]^{2+}$ core relative to the $[In_3Se_3]^{3+}$ core would be the stronger In--In coulombic repulsion due to the closer proximity of the two In^{3+} atoms in the former. This repulsive force is somewhat dissipated in $[In_3Se_3(Se_4)_3]^{3-}$ due to the longer In--In distances in the corresponding $[In_3Se_3]^{3+}$ core (3.336 Å vs 3.69 Å; vide infra). Thus, it is reasonable to propose a solution rearrangement of $[In_2Se_2(Se_4)_2]^{2-}$ to the more stable $[In_3Se_3(Se_4)_3]^{3-}$ as depicted in eq 8.

$$3[In_2Se_2(Se_4)_2]^{2-} \leftrightarrow 2[In_3Se_3(Se_4)_3]^{3-} \quad (8)$$

These equilibria also explain the similarity of the UV/vis spectra and the cyclic voltammetric data to those obtained from pure Se_x^{2-} solutions.

Solutions of $(Et_4N)_3[Tl_3Se_3(Se_4)_3]$ (VII) in DMF, acetonitrile and pyridine were also investigated by ^{77}Se NMR spectroscopy in the temperature range of 25 to –55 °C. At room temperature they show two broad triplets in the vicinity of 650 and 230 ppm, respectively. At –55 °C the spectra reveal nine sharp peaks of which only three are intense at 640, 273 and 218 ppm, respectively, as shown in Figure 5. These three peaks can be assigned to the $[Tl_3Se_3(Se_4)_3]^{3-}$ anion by analogy to the $[In_3Se_3(Se_4)_3]^{3-}$ anion. The peak at 640 ppm can be tentatively assigned to resonance from the terminal Se atoms of the chelating Se_4^{2-} ligands, the resonance at 273 ppm from the inner atoms of the Se_4^{2-} ligands and the 218 ppm is assigned to the Se^{2-} ligand. The ^{77}Se NMR spectra of (VII) in acetonitrile exhibits similar features at room temperature but at –40 °C only three main peaks are observed at 646, 271 and 216 ppm. In pyridine the spectra are similar to those in DMF at room temperature and again at –55 °C

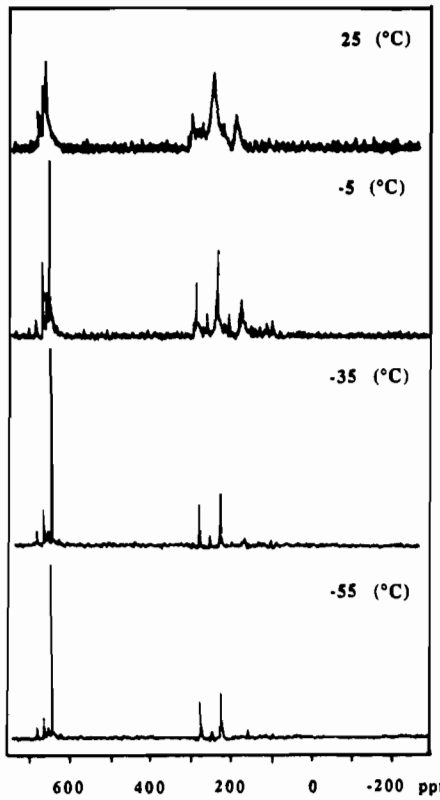

Figure 5. ^{77}Se NMR spectra of $(Et_4N)_3[Tl_3Se_3(Se_4)_3]$ (VII) in DMF as a function of temperature.

Table XI. Infrared Frequencies (cm^{-1}) of the Spectral Absorptions of (I)–(IV), (VI), and (VII)

complexes	frequencies (cm^{-1})
$(Ph_4P)_4[In_2(Se_4)_4(Se_5)]$	274 (w), 256 (m), 197 (s), 188 (w), 168 (m)
$(Pr_4N)_4[In_2(Se_4)_4(Se_5)]$	265 (m), 257 (m), 199 (s), 188 (s), 167 (s), 156 (m)
$(Et_4N)_4[In_2(Se_4)_4(Se_5)]$	270 (m), 254 (m), 230 (m), 224 (m), 205 (s), 171 (m)
$(Pr_4N)_2[In_2Se_2(Se_4)_2]$	268 (m), 258 (m), 231 (s), 205 (s), 190 (s)
$(Et_4N)_3[In_3Se_3(Se_4)_3]$	268 (m), 256 (m), 230 (m), 225 (m), 205 (s), 172 (m)
$(Et_4N)_3[Tl_3Se_3(Se_4)_3]$	268 (m), 253 (m), 187 (s), 170 (s)

only three main peaks are observed at 654, 285 and 230 ppm slightly down field from the previous two solvents. These results indicate considerable lability of the Se atoms in the Se_4^{2-} chelate probably due to an existence of redox equilibria between Tl^{3+} and Tl^{+} species in solution at room temperature. At lower temperatures the equilibrium shifts considerably toward the $[Tl_3Se_3(Se_4)_3]^{3-}$ anion and the six weak peaks observed in the DMF solution could be attributed to other as yet unknown $TlSe_x^{n-}$ complexes present in solution.

Far-IR Studies. In the far-IR region all the complexes reported here exhibit (in the solid state) spectral absorptions due to Se–Se and/or M–Se stretching vibrations. Observed absorption frequencies of all the complexes except (V) are given in Table XI. The spectrum of (V) is not shown because of the large number of strong absorptions from the $[(Ph_3P)_2N]^+$ cation in the region (500–100 cm^{-1}), which severely overlap with the Se–Se and In–Se absorptions.

Generally, two spectral absorptions are observed around ~268 and ~256 cm^{-1}. These bands can be assigned to Se–Se stretching vibrations by comparison with the spectra of other known polyselenide complexes and with that of the unbound ligand $(Ph_4P)_2Se_5$[27c] ($\nu_{Se\text{-}Se}$ at 267 cm^{-1}) and various other compounds

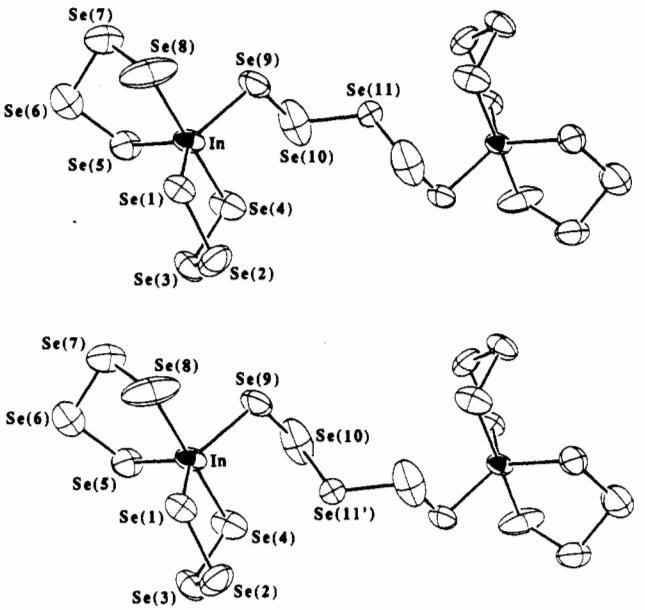

Figure 6. ORTEP representation of the two conformations of the $[In_2(Se_4)_4(Se_5)]^{4-}$ anion in (I) with labeling scheme.

e.g. Se_x^{2-} [42] ($x = 1$–6) at 258 cm^{-1}, c-Se_6[43] at 253 cm^{-1}, $[Fe_2Se_{12}]^{2-}$ [8] at 258 cm^{-1}, $[SnSe_{12}]^{2-}$ [26a] at 273 and 256 cm^{-1}, $[AgSe_x]^{-}$ [27c] (x = 4, 5) around 265 cm^{-1} and $[PdSe_8]^{2-}$ [14] at 247 cm^{-1}. In the In^{3+}/Se_x^{2-} complexes an additional strong band in the range 197–205 cm^{-1} is observed. This might be a possible candidate for an In–Se stretching vibration by comparison to the spectra of α-$In_2Se_3(H)$ and α-$In_2Se_3(R)$[44] which exhibit two strong absorptions at 188, 163 cm^{-1} and 189, 164 cm^{-1}, respectively. In the Tl^{3+}/Se_x^{2-} complex this absorption shifts to 170 cm^{-1} and could be due to a Tl-Se stretching vibration. The major difficulty in unequivocally assigning the observed IR absorptions of these complexes arises from the fact that the Se–Se and M–Se stretching frequencies fall in the same low-frequency region of 150–280 cm^{-1} for which systematic and quantitative studies are lacking.

Description of the Structures. Structure of $(Ph_4P)_4[In_2(Se_4)_4(Se_5)]$ (I). Figure 6 shows the structure of the $[In_2(Se_4)_4(Se_5)]^{4-}$ anion. It consists of two $[In(Se_4)_2]^-$ units bridged by a Se_5^{2-} chain. The In atom has a trigonal-bipyramidal coordination geometry. The metal atom is chelated by two Se_4^{2-} ligands and bound to a terminal Se atom of the Se_5^{2-} chain. Two axial selenium atoms Se(4) and Se(8) and the three equatorial atoms Se(1), Se(5) and Se(9) compose the coordination sphere of indium. The axial Se(4)–In–Se(8) angle is 175.7(1)°. The equatorial Se–In–Se angles average to 119.9(2)° and the In, Se(1), Se(5) and Se(9) atoms do not deviate more than 0.02 Å from the corresponding least-squares plane. All chelating Se_4^{2-} ligands adopt an envelope conformation. Atoms Se(3) and Se(7) are an average of 1.280(2) Å away from the InSe(1)Se(2)Se(4) and InSe(5)Se(6)Se(8) planes, respectively. The anion $[In_2(Se_4)_4(Se_5)]^{4-}$ itself does not have a center of symmetry, but a crystallographically imposed center of symmetry lies halfway between the In---In vector. This induces a positional disorder of the central Se(11) atom of the bridging Se_5^{2-} chain and results in two different conformations of the Se_5^{2-} chain in the solid state with a half-positional occupancy of the Se(11) atom as shown in Figure 6. Selected bond distances and angles are given in Table XII.

(42) Weller, F.; Adel, J.; Dehnicke, K. *Z. Anorg. Allg. Chem.* **1987**, *548*, 125–132.
(43) Nagata, K.; Tshibashi, K.; Miyamoto, Y. *Jpn. J. Appl. Phys.* **1980**, *19*, 1569–1573.
(44) Lutz, H. D.; Fischer, M.; Baldus, H.-P.; Blanchnik, R. *J. Less-Common Met.* **1988**, *143*, 83–92.

Table XII. Comparison of Selected Bond Distances (Å) and Bond Angles (deg) of the $[In_2(Se_4)_4(Se_5)]^{4-}$ Anion in (I)–(III) with Standard Deviations in Parentheses

	(I)	(II)	(III)		(I)	(II)	(III)
In–Se(1)	2.663(3)	2.799(4)	2.614(4)	Se(4)–In–Se(9)	93.5(2)	90.9(2)	95.6(1)
In–Se(4)	2.729(3)	2.639(5)	2.677(4)	Se(5)–In–Se(8)	98.1(2)	99.2(2)	98.3(1)
In–Se(5)	2.622(3)	2.552(5)	2.608(5)	Se(5)–In–Se(9)	117.1(2)	121.6(2)	122.9(2)
In–Se(8)	2.735(3)	2.852(6)	2.890(4)	Se(8)–In–Se(9)	87.4(2)	84.0(2)	74.9(1)
In–Se(9)	2.616(3)	2.692(5)	2.608(4)	Se(13)–In(2)–Se(14)			94.4(1)
In(2)–Se(13)			2.613(5)	Se(13)–In(2)–Se(17)			126.7(2)
In(2)–Se(14)			2.708(5)	Se(13)–In(2)–Se(18)			113.4(2)
In(2)–Se(17)			2.612(5)	Se(13)–In(2)–Se(21)			79.8(2)
In(2)–Se(18)			2.615(5)	Se(14)–In(2)–Se(17)			98.6(2)
In(2)–Se(21)			2.815(6)	Se(14)–In(2)–Se(18)			93.3(2)
In–Se(mean)	2.67(5)	2.7(1)	2.68(9)	Se(14)–In(2)–Se(21)			169.2(2)
Se(1)–Se(2)	2.331(7)	2.245(6)	2.353(6)	Se(17)–In(2)–Se(18)			117.1(2)
Se(2)–Se(3)	2.334(5)	2.446(6)	2.321(5)	Se(17)–In(2)–Se(21)			78.2(2)
Se(3)–Se(4)	2.349(6)	2.412(6)	2.322(5)	Se(18)–In(2)–Se(21)			97.4(2)
Se(5)–Se(6)	2.312(8)	2.177(6)	2.318(6)	In–Se(1)–Se(1)	103.8(2)	98.3(2)	101.6(2)
Se(6)–Se(7)	2.290(7)	2.436(7)	2.313(6)	Se(1)–Se(2)–Se(3)	100.9(2)	103.9(2)	92.8(2)
Se(7)–Se(8)	2.337(5)	2.251(7)	2.327(6)	Se(2)–Se(3)–Se(4)	99.1(2)	105.7(2)	99.7(2)
Se(9)–Se(10)	2.383(9)	2.46(1)	2.352(6)	In–Se(4)–Se(3)	96.0(2)	84.3(2)	97.7(2)
Se(9)–Se(10′)		2.21(1)		In–Se(5)–Se(6)	103.9(2)	93.3(2)	102.8(2)
Se(10)–Se(11)	2.322(9)	2.56(1)	2.334(7)	Se(5)–Se(6)–Se(7)	102.5(2)	99.8(2)	102.3(2)
Se(10′)–Se(11)		2.45(1)		Se(6)–Se(7)–Se(8)	102.7(2)	101.5(2)	101.8(2)
Se(11)–Se(12)			2.310(6)	In–Se(8)–Se(7)	97.6(2)	96.6(2)	102.6(2)
Se(12)–Se(13)			2.353(6)	In–Se(9)–Se(10)	103.6(2)	106.5(3)	103.2(2)
Se(14)–Se(15)			2.329(6)	In–Se(9)–Se(10′)		110.5(3)	
Se(15)–Se(16)			2.341(7)	Se(9)–Se(10)–Se(11)	113.7(3)	114.6(5)	105.8(2)
Se(16)–Se(17)			2.340(8)	Se(9)–Se(10′)–Se(11′)		110.9(5)	
Se(18)–Se(19)			2.305(8)	Se(10)–Se(11)–Se(10′)		117.6(5)	
Se(19)–Se(20)			2.317(8)	Se(10)–Se(11)–Se(12)			104.5(2)
Se(20)–Se(21)			2.318(9)	In(2)–Se(13)–Se(12)			100.6(2)
Se–Se(mean)	2.33(2)	2.36(1)	2.33(2)	In(2)–Se(14)–Se(15)			96.0(2)
				In(2)–Se(17)–Se(16)			103.5(2)
Se(1)–In–Se(4)	96.6(2)	105.3(1)	100.7(1)	In(2)–Se(18)–Se(19)			104.0(2)
Se(1)–In–Se(5)	118.9(2)	104.8(2)	109.2(1)	In(2)–Se(21)–Se(20)			98.2(2)
Se(1)–In–Se(8)	79.4(2)	69.3(1)	77.7(1)	Se(14)–Se(15)–Se(16)			100.5(2)
Se(1)–In–Se(9)	123.6(1)	129.6(2)	123.5(1)	Se(15)–Se(16)–Se(17)			101.4(2)
Se(4)–In–Se(5)	85.3(2)	94.2(2)	94.6(2)	Se(18)–Se(19)–Se(20)			103.0(3)
Se(4)–In–Se(8)	175.7(1)	166.4(2)	166.8(1)	Se(19)–Se(20)–Se(21)			102.2(3)

Structure of $(Pr_4N)_4[In_2(Se_4)_4(Se_5)]$ (II). The anion in this compound is similar to (I) i.e. $[In_2(Se_4)_4(Se_5)]^{4-}$ where the trigonal bipyramidal In^{3+} center is chelated by two Se_4^{2-} ligands and a terminal selenium atom of a Se_5^{2-} chain bridging the two In atoms. The axial Se(4)–In–Se(8) angle is 166.4(2)° and the corresponding equatorial Se–In–Se angles average 118.7(2)°. The chelating Se_4^{2-} ligands adopt an envelope conformation. Atoms Se(3) and Se(6) are an average 1.36 Å away from the InSe(1)Se(2)Se(4) and InSe(5)Se(7)Se(8) planes, respectively. There is a crystallographic C_2 axis passing through the middle of the In---In vector. The C_2 axis passes close to the Se(11) and thus giving rise to disorder. The Se(10) is also disordered, and hence, the bridging Se_5^{2-} chain has two different conformations in the solid state as shown in Figure 7. Due to the marginal quality of the data set, the accuracy of the Se--Se bonds in the Se_5^{2-} chain is low. Selected bond distances and angles are given in Table XII.

Structure of $(Et_4N)_4[In_2(Se_4)_4(Se_5)]$ (III). The anion is similar to (I) and (II) as it contains the same structural unit $[In_2(Se_4)_4(Se_5)]^{4-}$ without disorder, shown in Figure 8. The average angle between Se_{ax}–In–Se_{ax} is 168.0(2)°. The axial Se ligands are Se(4), Se(8) and Se(14), Se(21) for In(1) and In(2), respectively. The corresponding equatorial angles average 118.8(2)°. The In atoms deviate an average of 0.24 Å from the equatorial selenium atoms. The two chelating Se_4^{2-} ligands adopt an envelope conformation similar to the one seen in (I) and (II). Atoms Se(3), Se(6), Se(15) and Se(20) lie an average of 1.260(3) Å away from the basal planes. In the bridging Se_5^{2-} chain Se(11) lies 1.38 Å away from the Se(9), Se(10), Se(12) and Se(13) plane. The atoms in this plane do not deviate more than 0.013 Å from the least-squares plane. Selected bond distances and angles are given in Table XII.

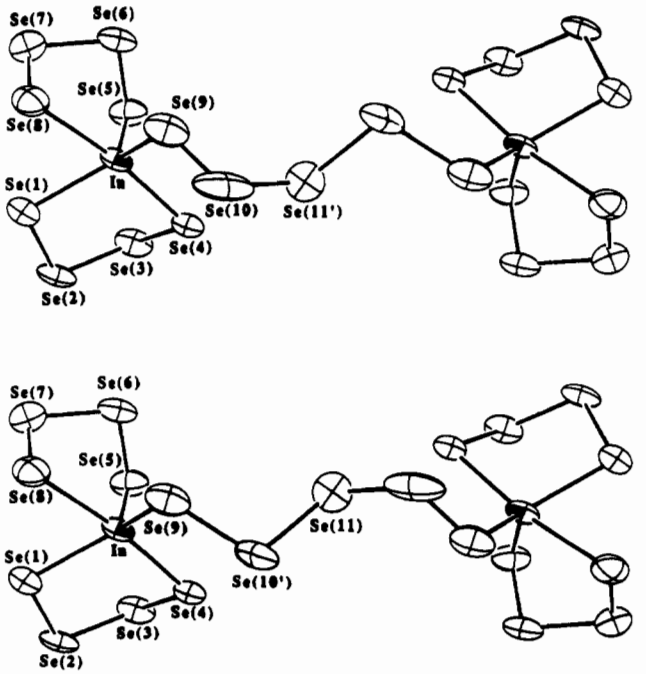

Figure 7. ORTEP representation of the two conformations of the $[In_2(Se_4)_4(Se_5)]^{4-}$ anion in (II) with labeling scheme.

Structure of $(Pr_4N)_2[In_2Se_2(Se_4)_2]$ (IV). The binuclear anion $[In_2Se_2(Se_4)_2]^{2-}$ contains In^{3+} with a tetrahedral coordination, bridged by two selenides to form a planar $[In_2Se_2]^{2+}$ core which sits on an inversion center. The nonbonding In--In distance is 3.336(2) Å. The remaining two coordination sites on each In atom are occupied by the Se_4^{2-} bidentate chelates as shown in

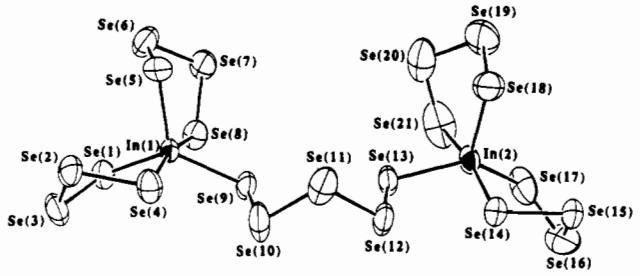

Figure 8. ORTEP representation of the $[In_2(Se_4)_4(Se_5)]^{4-}$ anion in (III) with labeling scheme.

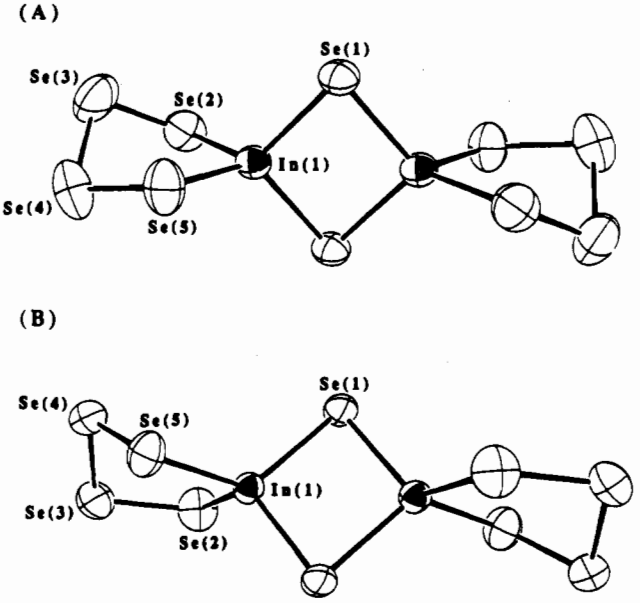

Figure 9. ORTEP representation and labeling scheme of the $[In_2Se_2(Se_4)_2]^{2-}$ anions in (A) $(Pr_4N)_2[In_2Se_2(Se_4)_2]$ and (B) $[(Ph_3P)_2N]_2[In_2Se_2(Se_4)_2]$.

Figure 9A. The In--Se bonds in the core are shorter (av 2.564(4) Å) than in the $InSe_4$ rings (av 2.606(4) Å) where as the In–Se(1)–In′ angle is 81.2° and the Se(1)-In-Se(1)′ is 98.8° in the $[In_2Se_2]^{2+}$ core. The Se_4^{2-} ligand adopts a twisted half-boat conformation with the Se(3) and Se(4) atoms lying an average of 0.725(1) Å above and below, respectively, from the In Se(2) Se(5) basal plane. Selected bond distances and angles are given in Table XIII.

Structure of $[(Ph_3P)_2N]_2[In_2Se_2(Se_4)_2]$ (V). The anion moiety of (V) is similar to (IV) as it contains the same structural unit as $[In_2Se_2(Se_4)_2]^{2-}$. However, in this anion the Se_4^{2-} ligand adopts an envelop conformation with In, Se(2), Se(3), Se(5) atoms in a least-square plane with the mean deviation of 0.052 Å and the Se(4) lying 1.197 Å away from the plane as shown in Figure 9B. Selected bond distances and angles of the anion are compared with those of (IV) in Table XIII.

Structure of $(Et_4N)_3[In_3Se_3(Se_4)_3]$ (VI). The trinuclear anion $[In_3Se_3(Se_4)_3]^{3-}$, is shown in Figure 10 and contains In^{3+} with a tetrahedral coordination. Each In^{3+} center has a chelating Se_4^{2-} ligand and is bridged to the other two In^{3+} centers by monoselenide, Se^{2-}, ligands. The bridging Se^{2-} leads to an interesting six-membered ring as the core of the anionic structure consisting of alternating In and Se atoms. This $[In_3Se_3]^{3+}$ core has a distorted boat conformation. The average In---In distance is 3.689(2) Å. There is a least-squares plane defined by the In(1), In(2), In(3) and Se(15) atoms of the $[In_3Se_3]^{3+}$ core with the average deviation of the four atoms from the least squares plane of 0.104 Å. Se(5) and Se(10) lie 1.796 and 1.544 Å above and below this plane, respectively. The In--Se bonds in the six-membered $[In_3Se_3]^{3+}$ ring are shorter (av 2.561(15) Å) than the In--Se bonds in the $InSe_4$ rings (av 2.620(17) Å). Within the $[In_3Se_3]^{3+}$ core, the average In–Se–In angle is 92.2° while the average Se–In–Se is 111.4°. The chelating Se_4^{2-} ligands adopt two different conformations. The In(1) atom is coordinated with a Se_4^{2-} in a half-twist conformation where as In(2) and In(3) atoms have the ligands in the envelop conformation. In the twist half-boat conformation the Se(2) and Se(3) atoms lie at an average 0.711 Å away from the In(1)Se(1)Se(4) plane. Atoms Se(8) and Se(13) lie an average of 1.332(2) Å away from the In(2)Se(6)Se(7)Se(9) and In(3)Se(11)Se(12)Se(14) basal planes, respectively. The disorder in one of the Se_4^{2-} ligands chelating to In(2) atom leads to two conformations of the Se_4^{2-} bidentate in the solid state, as shown in Figure 10. Selected bond distances and angles are given in Table XIV.

Table XIII. Comparison of Selected Bond Distances (Å) and Bond Angles (deg) of the $[In_2Se_2(Se_4)_2]^{2-}$ Anion in (IV) and (V) with Standard Deviations in Parentheses

	$(Pr_4N)_2$-$[In_2Se_2(Se_4)_2]$	$[(Ph_3P)_2N]_2$-$[In_2Se_2(Se_4)_2]$
In–In′	3.336(2)	3.347(4)
In–Se(1)	2.565(2)	2.557(4)
In–Se(1′)	2.562(2)	2.571(4)
In–Se(2)	2.602(2)	2.617(4)
In–Se(5)	2.609(2)	2.605(4)
In–Se(mean)	2.585(8)	2.588(12)
Se(2)–Se(3)	2.325(3)	2.325(5)
Se(3)–Se(4)	2.340(4)	2.307(5)
Se(4)–Se(5)	2.320(3)	2.321(5)
Se–Se(mean)	2.328(10)	2.318(12)
Se(1)–In–Se(1′)	98.80(6)	98.5(1)
Se(1)–In–Se(2)	109.73(8)	105.4(1)
Se(1)–In–Se(5)	120.20(8)	121.3(1)
Se(2)–In–Se(1′)	120.19(8)	119.9(1)
Se(2)–In–Se(5)	103.47(8)	103.0(1)
Se(5)–In–Se(1′)	105.49(7)	109.8(1)
In–Se(1)–In′	81.20(6)	81.5(1)
In–Se(2)–Se(3)	95.9(1)	99.7(2)
Se(2)–Se(3)–Se(4)	100.8(1)	103.5(2)
Se(3)–Se(4)–Se(5)	100.7(1)	102.7(2)
Se(4)–Se(5)–In	97.96(9)	96.2(2)

Structure of $(Et_4N)_3[Tl_3Se_3(Se_4)_3]$ (VII). The structure of the $[Tl_3Se_3(Se_4)_3]^{3-}$ anion is identical to its indium analog. This structure shows no disorder in any of its $TlSe_4$ rings. Selected bond distances and angles are compared with those of the In analog in Table XIV.

Comparison of Structures. Prior to our work in the In/Se_x system there was only one known soluble molecular compound, $In_4Se_{10}^{8-}$, isolated by Krebs and co-workers.[45] It contains tetrahedral In^{3+} centers with bridging and terminal Se^{2-} ligands forming a small adamantoid unit. Indium has mainly been found coordinated to selenide ligands either tetrahedrally (e.g. $CuInSe_2$,[46] $In_4Se_{10}^{8-}$,[45] $Rb_4In_2Se_5$,[47] $Ba_2In_2Se_5$,[48] $KInSe_2$[49]) or octahedrally (e.g. $NaInSe_2$,[50] Pr_3InSe_6[51]). Five coordination by selenium-only ligands found in $[In_2(Se_4)_4(Se_5)]^{4-}$ is in fact rare. The trigonal-bipyramidal geometry around the In atom can be rationalized in terms of valence shell electron pair repulsion (VSEPR) theory. In (I)–(III) In^{3+} atoms are found in a trigonal-bipyramidal coordination and the average In–Se bond lengths in these complexes are 2.673, 2.707, and 2.676 Å, respectively. In comparison, the In–Se distance in the tetrahedrally coordinated In^{3+} complexes (IV)–(VI) are an average 0.096 Å shorter compared with the average In–Se bond distance of 2.585, 2.588,

(45) Krebs, B.; Voelker, D.; Stiller, K. O. *Inorg. Chim. Acta* **1982**, *65*, L101–L102.
(46) Parkes, J.; Tomlinson, R. D.; Hampshire, M. J. *J. Appl. Crystallogr.* **1973**, 414–416.
(47) Krebs, B *Angew. Chem., Int. Ed. Engl.* **1983**, *22*, 113–134.
(48) Eisenmann, B.; Hofmann, A. *Z. Anorg. Allg. Chem.* **1990**, *580*, 151–159.
(49) Krebs, B.; Stiller, K. O. Unpublished results (in ref 47).
(50) Hoppe, R.; Lidecke, W.; Frorath, F.-C. *Z. Anorg. Allg. Chem.* **1961**, *309*, 49–54.

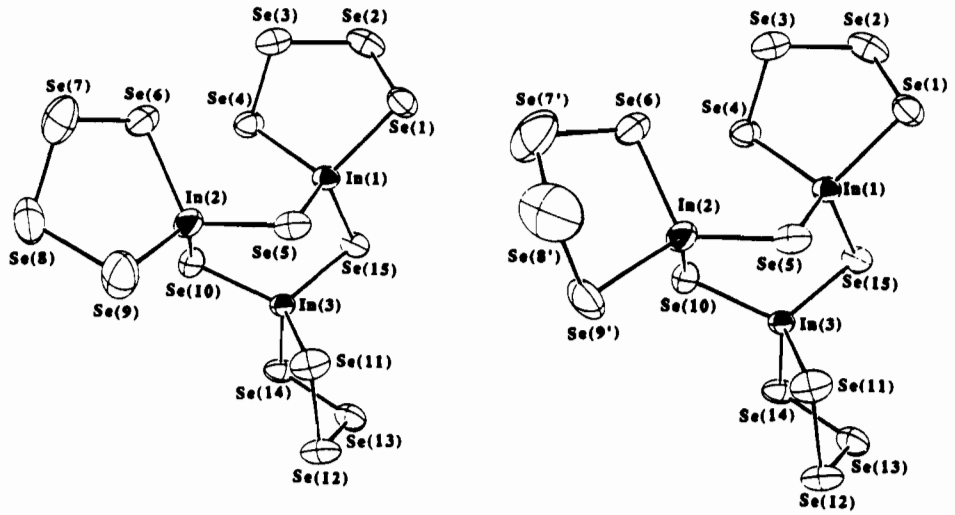

Figure 10. ORTEP representation of the $[In_3Se_3(Se_4)_3]^{3-}$ anion in (VI) with labeling scheme. Two conformations found in one of the Se_4^{2-} ligands bonded to In(2) are shown. The structure of $[Tl_3Se_3(Se_4)_3]^{3-}$ is identical to that of the left.

Table XIV. Comparison of Selected Bond Distances (Å) and Bond Angles (deg) of the $[M_3Se_3(Se_4)_3]^{3-}$ Anion in (VI) and (VII) with Standard Deviations in Parentheses

	$(Et_4N)_3[In_3Se_3(Se_4)_3]$	$(Et_4N)_3[Tl_3Se_3(Se_4)_3]$		$(Et_4N)_3[In_3Se_3(Se_4)_3]$	$(Et_4N)_3[Tl_3Se_3(Se_4)_3]$
M(1)–M(2)	3.665(2)	3.656(3)	Se(4)–M(1)–Se(15)	115.9(1)	106.7(2)
M(1)–M(3)	3.591(2)	3.734(3)	Se(5)–M(1)–Se(15)	110.6(1)	110.8(2)
M(2)–M(3)	3.811(2)	3.886(3)	Se(5)–M(2)–Se(6)	113.7(1)	108.5(2)
av M- -M	3.69(9)	3.76(9)	Se(5)–M(2)–Se(9)	100.2(1)	107.2(2)
M(1)–Se(1)	2.621(3)	2.681(5)	Se(5)–M(2)–Se(9′)	117.8(2)	
M(1)–Se(4)	2.602(3)	2.659(6)	Se(5)–M(2)–Se(10)	110.5(1)	113.4(2)
M(1)–Se(5)	2.576(3)	2.585(5)	Se(6)–M(2)–Se(9)	102.5(1)	100.2(2)
M(1)–Se(15)	2.537(3)	2.639(5)	Se(6)–M(2)–Se(9′)	101.3(2)	
M(2)–Se(5)	2.543(3)	2.627(6)	Se(6)–M(2)–Se(10)	109.8(1)	110.2(2)
M(2)–Se(6)	2.632(3)	2.668(6)	Se(9)–M(2)–Se(10)	120.0(1)	116.4(2)
M(2)–Se(9)	2.627(6)	2.666(5)	Se(9′)–M(2)–Se(10)	103.1(3)	
M(2)–Se(9′)	2.65(1)		Se(10)–M(3)–Se(11)	116.1(1)	117.5(2)
M(2)–Se(10)	2.567(4)	2.629(6)	Se(10)–M(3)–Se(14)	107.0(1)	107.7(2)
M(3)–Se(10)	2.577(3)	2.628(7)	Se(10)–M(3)–Se(15)	113.0(1)	111.0(2)
M(3)–Se(11)	2.595(3)	2.670(9)	Se(11)–M(3)–Se(14)	101.5(1)	101.3(2)
M(3)–Se(14)	2.610(3)	2.686(6)	Se(11)–M(3)–Se(15)	110.1(1)	105.5(2)
M(3)–Se(15)	2.565(3)	2.586(6)	Se(14)–M(3)–Se(15)	108.3(1)	113.6(2)
M–Se(mean)	2.59(3)	2.64(3)	M(1)–Se(1)–Se(2)	97.0(1)	97.0(2)
Se(1)–Se(2)	2.346(4)	2.351(8)	Se(1)–Se(2)–Se(3)	101.8(1)	102.6(3)
Se(2)–Se(3)	2.330(4)	2.333(8)	Se(2)–Se(3)–Se(4)	101.1(1)	101.1(3)
Se(3)–Se(4)	2.337(4)	2.323(8)	M(1)–Se(4)–Se(3)	97.4(1)	89.1(2)
Se(6)–Se(7)	2.419(5)	2.324(8)	M(1)–Se(5)–M(2)	91.4(1)	91.4(1)
Se(6)–Se(7′)	2.27(1)		M(2)–Se(6)–Se(7)	99.2(2)	93.9(2)
Se(7)–Se(8)	2.319(7)	2.325(8)	Se(6)–Se(7)–Se(8)	101.7(2)	100.2(3)
Se(7′)–Se(8′)	2.29(2)		Se(6)–Se(7′)–Se(8′)	101.1(6)	
Se(8)–Se(9)	2.343(7)	2.359(8)	Se(7)–Se(8)–Se(9)	100.7(2)	101.8(3)
Se(8′)–Se(9′)	2.27(2)		Se(7′)–Se(8′)–Se(9′)	105.4(7)	
Se(11)–Se(12)	2.369(4)	2.265(12)	M(2)–Se(9)–Se(8)	95.0(2)	100.2(2)
Se(12)–Se(13)	2.320(4)	2.271(13)	M(2)–Se(9′)–Se(8′)	90.6(5)	
Se(13)–Se(14)	2.328(4)	2.371(10)	M(2)–Se(10)–M(3)	95.7(1)	95.3(2)
Se–Se(mean)	2.33(4)	2.33(4)	M(3)–Se(11)–Se(12)	100.4(1)	97.7(4)
			Se(11)–Se(12)–Se(13)	101.8(1)	105.8(4)
Se(1)–M(1)–Se(4)	103.9(1)	102.1(2)	Se(12)–Se(13)–Se(14)	99.6(1)	105.2(4)
Se(1)–M(1)–Se(5)	110.7(1)	109.6(2)	M(3)–Se(14)–Se(13)	93.7(1)	99.5(3)
Se(1)–M(1)–Se(15)	109.1(1)	110.5(2)	M(1)–Se(15)–M(3)	89.5(1)	91.3(2)
Se(4)–M(1)–Se(5)	106.6(1)	116.9(2)			

and 2.593 Å, respectively. This decrease in the bond lengths is as expected, going from five-coordinate to a four-coordinate geometry. The bond distances are shorter as expected, than the average In–Se distance in an octahedral coordination, at 2.722 Å (e.g. Pr_3InSe_6[51]).

The dimeric structure of the anion in (I)–(III) resembles that of $[Bi_2(S_7)_4S_6]^{4-}$,[52] which is composed of two highly distorted square-pyramidal $[Bi(S_7)_2]^-$ units bridged by a S_6^{2-} chain. Examples of a single polychalcogenide Q_x^{2-} chain bridging two separate M/Q_x units are observed in $[Cu_2Se_{14}]^{4-}$,[24] $[Ag_2S_{20}]^{4-}$,[53] and $[Cu_2S_{20}]^{4-}$,[54] which have bridging Se_5^{2-} and S_8^{2-}, respectively.

The anions in (IV) and (V) consist of a $[In_2Se_2]^{2+}$ core where as (VI) and (VII) contain a $[M_3Se_3]^{3+}$ (M = In, Tl) core, and the overall structures are homologous not only to each other but also to those of $[Au_2Se_2(Se_4)_2]^{2-}$ [22] and $[Fe_2Se_2(Se_5)_2]^{2-}$.[8] The $[In_2Se_2]^{2+}$ core was also found in $Rb_4In_2Se_5$,[47] $Ba_2In_2Se_5$[48] with similar dimensions. It is interesting to note that the dimeric

(51) Aleandri, L. E.; Ibers, J. A. *J. Solid State Chem.* **1989**, *79*, 107–111.
(52) Müller, A.; Zimmermann, M.; Bögge, H. *Angew. Chem., Int. Ed. Engl.* **1986**, *25*, 273–274.
(53) Müller, A.; Krickemeyer, E.; Zimmermann, M.; Römer, M.; Bögge, H.; Penk, M.; Schmitz, K. *Inorg. Chim. Acta* **1984**, *90*, L69–L70.
(54) Müller, A.; Baumann, F.-W.; Bögge, H.; Römer, M.; Krickemeyer, E.; Schmitz, K. *Angew. Chem., Int. Ed. Engl.* **1984**, *23*, 632–633.

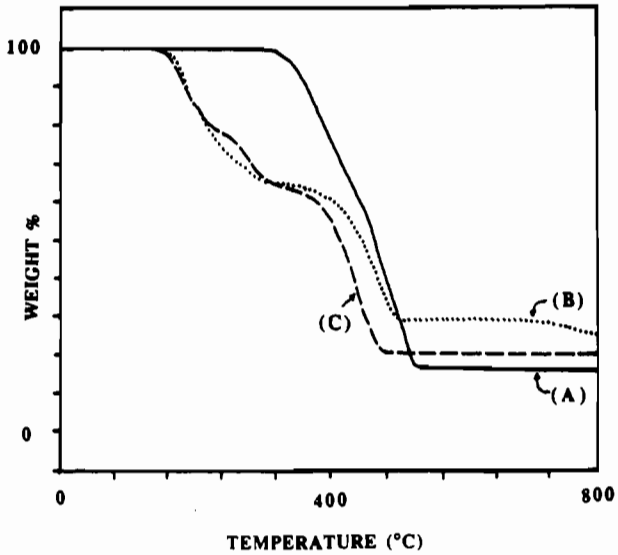

Figure 11. TGA diagrams (under nitrogen) of (A) $(Ph_4P)_4[In_2(Se_4)_4(Se_5)]$ (I), (B) $(Pr_4N)_4[In_2(Se_4)_4(Se_5)]$ (II), and (C) $(Et_4N)_4[In_2(Se_4)_4(Se_5)]$ (III). The final product in these cases is β-In_2Se_3.

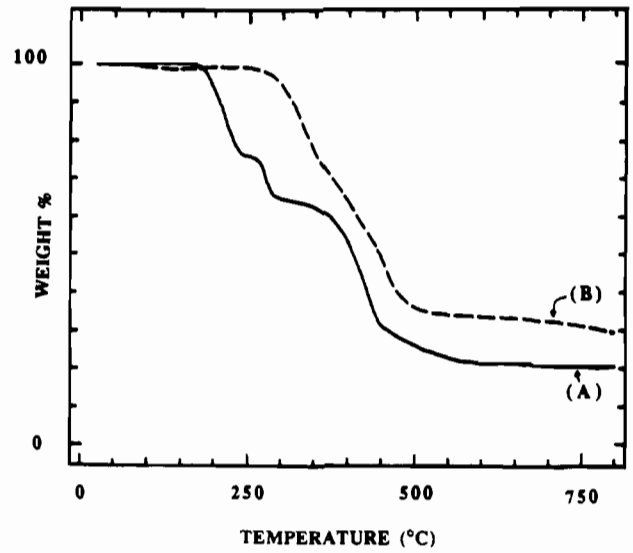

Figure 12. TGA diagrams (under nitrogen) of (A) $(Pr_4N)_2[In_2Se_2(Se_4)_2]$ (IV) and (B) $[(Ph_3P)_2N]_2[In_2Se_2(Se_4)_2]$ (V).

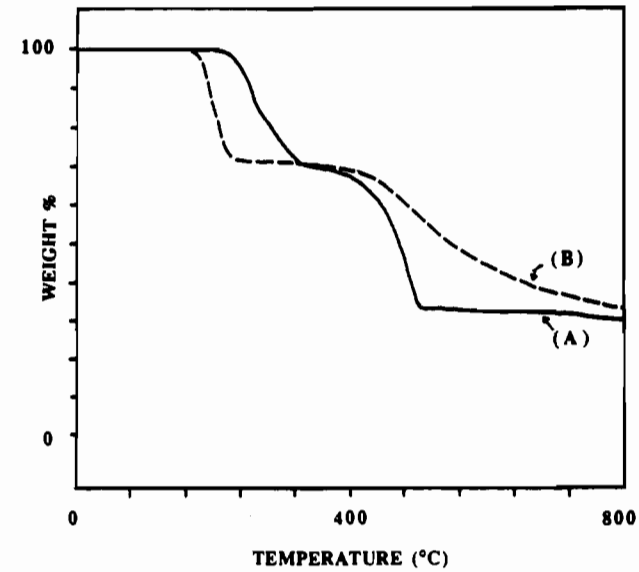

Figure 13. TGA diagrams (under nitrogen) of (A) $(Et_4N)_3[In_3Se_3(Se_4)_3]$ (VI) and (B) $(Et_4N)_3[Tl_3Se_3(Se_4)_3]$ (VII).

$[In_2Se_2(Se_4)_2]^{2-}$ anions in (IV) and (V) have been stabilized by large organic countercations while the trimeric $[M_3Se_3(Se_4)_3]^{3-}$ anions by the smaller Et_4N^+ cations. This is the result of the packing forces in the crystal lattice which are greatly influenced by the size of the counter ions. A definite trend by which counterions affect the structures of anionic M/Q_x complexes is not yet established but some preferences have been identified.[27,36c]

Except for $[Fe_2Se_2(Se_5)_2]^{2-}$ the most preferred polyselenide ligand size for chelation is Se_4^{2-}. Although there seems to be no systematic trend as to why some metals prefer Se_5^{2-} and some Se_4^{2-}, we note that $(Ph_4P)_2[Ga_2Se_2(Se_5)_2]$,[55] which is isostructural to the Fe compound, contains Se_5^{2-}, suggesting a mild M^{n+} size dependence in which small ions prefer to bind chelating Se_5^{2-} ligands. However, more studies are needed to confirm such a relationship.

Our inability to synthesize $[In(Se_4)_2]^-$ (isostructural to $[Zn(Se_4)_2]^{2-}$ [15,16]) from DMF, acetonitrile, or water may originate in the fact that this hypothetical anion has a single negative charge and thus requires only one cation to balance it. A single cation for each anion in the crystal lattice may not be able to effectively screen all $[In(Se_4)_2]^-$ anions from each other (as it is possible with $[Zn(Se_4)_2]^{2-}$) and Coulombic repulsions could destabilize the lattice.[36c] It is interesting to note that there are no mononuclear molecular $[M(Q_x)_2]^-$ complexes. The recently reported $(R_4E)[M(Q_x)_2]$ are shown to be polymeric.[56]

Thermal Decomposition Studies. All compounds were studied by thermal gravimetric analysis (TGA). The temperature at which these complexes start to lose weight (and presumably start to decompose) depends on the nature of the counterions. The indium polyselenides decompose to form β-In_2Se_3 as the final product as identified by X-ray diffraction. During pyrolysis, the complexes lose R_3P or R_3N, R_3PSe, R_2Se and elemental Se. The TGA diagram of $(Ph_4P)_4[In_2(Se_4)_4(Se_5)]$ (I) does not show any appreciable weight loss below 350 °C. A continuous weight loss is observed from 350 to 530 °C. In contrast, this behavior is not shared by (II) and (III) which contain Pr_4N^+ and Et_4N^+, respectively. The TGA curves are shown in Figure 11. (III) begins to lose weight around 145 °C exhibiting a well-defined two-step weight loss and stabilizing at around 500 °C. (II) begins to lose weight around 135 °C and exhibits a three-step weight loss up to 480 °C. The thermal stability of the complexes is in the order $Ph_4P^+ > Pr_4N^+ > Et_4N^+$. This trend directly reflects the order of susceptibility of nucleophilic attack on the organic cations by the selenide ligands, taking into consideration the stabilities of the alkyl--N and aryl--P bonds in these cations. (IV) and (V) exhibit rather complicated weight loss from 180 to 570 °C and 260 to 900 °C, respectively. Interestingly (VI) shows a higher thermal stability and losses weight from 205 to 500 °C. The TGA curves of (IV)–(VII) are shown in Figures 12 and 13.

The Tl^{3+} polyselenide (VII) starts to decompose at 190 °C and the final product, at a temperature above 500 °C, was identified by powder X-ray diffraction pattern as TlSe.[57] The final weight loss observed from the TGA curves of all complexes are in good agreement with the expected theoretical values for the corresponding binary metal selenides. This property suggests a possible use of these compounds as precursors to thin films of the corresponding binary selenides.[28]

Conclusion

The reaction of alkali metal polyselenides with indium trichloride in the presence of various organic cations in different

(55) Dhingra, S.; Kanatzidis M. G. Unpublished results. The reaction of $GaCl_3$ with 2 equiv of Na_2Se_4 in the presence of 1 equiv Ph_4PCl in DMF afforded red crystals of $(Ph_4P)_2[Ga_2Se_2(Se_5)_2]$ in 72% yield. This complex crystallizes in the monoclinic space group $C2/c$ with unit cell dimensions a = 22.288(5) Å, b = 16.491(7) Å, c = 16.064(3) Å, β = 104.99(2)°, V = 5703(3)Å^3, and Z = 4: Dhingra, S. Ph.D. Dissertation, Michigan State University, 1992.

(56) Dhingra, S.; Kanatzidis M. G. *Science* **1993**, *258*, 1769–1772.

(57) JCPDS Powder Diffraction File: (TlSe)16*U* No. 22-1476; International Center for Diffraction Data, 1983, Swarthmore, PA.

solvents affords several new In^{3+} polyselenide complexes: $(Ph_4P)_4[In_2(Se_4)_4(Se_5)]$, $(Pr_4N)_4[In_2(Se_4)_4(Se_5)]$, $(Et_4N)_4[In_2(Se_4)_4(Se_5)]$, $(Pr_4N)_2[In_2Se_2(Se_4)_2]$, $[(Ph_3P)_2N]_2[In_2Se_2(Se_4)_2]$, and $(Et_4N)_3[In_3Se_3(Se_4)_3]$. Similar reaction of thallium(I) chloride with pentaselenide anion, Se_5^{2-}, in the presence of Et_4NBr results in the first thallium(III) polyselenide: $(Et_4N)_3[Tl_3Se_3(Se_4)_3]$. In this system the stabilization of anionic species seems to depend first on the solvent and second on the size of the organic cations. The hydrothermal technique is a valuable tool in crystallizing novel compounds often not accessible by the more classical room-temperature solution technique and thus it is complementary to it. The indium polyselenide complexes (I)–(VI) convert to a single In/Se_x species, which attests to the facile and complex equilibria operating between the different In/Se species in polar solvents. The complexes decompose to β-In_2Se_3 and TlSe and suggest application as low-temperature precursors to films of these solid-state materials.[28]

Acknowledgment. Financial support from the donors of the Petroleum Research Fund, administered by the American Chemical Society, and by the National Science Foundation for a Presidential Young Investigator Award is gratefully acknowledged. The NMR data were obtained on instrumentation purchased in part with funds from NIH Grant 1-S10-RR04750-01 and from an NSF Grant CHE-88-00770. The single-crystal X-ray diffractometers used in this work were purchased by a grant from the National Science Foundation (CHE-8908088).

Supplementary Material Available: Tables of crystallographic data, calculated and observed X-ray powder diffraction patterns, atomic coordinates of all atoms, and anisotropic and isotropic thermal parameters of all non-hydrogen atoms for $(Ph_4P)_4[In_2(Se_4)_4(Se_5)]$ (**I**), $(Pr_4N)_4[In_2(Se_4)_4(Se_5)]$ (**II**), $(Et_4N)_4[In_2(Se_4)_4(Se_5)]$ (**III**), $(Pr_4N)_2[In_2Se_2(Se_4)_2]$ (**IV**), $[(Ph_3P)_2N]_2[In_2Se_2(Se_4)_2]$ (**V**), $(Et_4N)_3[In_3Se_3(Se_4)_3]$ (**VI**), and $(Et_4N)_3[Tl_3Se_3(Se_4)_3]$ (**VII**) (62 pages). Ordering information is given on any current masthead page.